

CERN-EP/2016-073
2016/09/09

CMS-FSQ-13-008

Evidence for exclusive $\gamma\gamma \rightarrow W^+W^-$ production and constraints on anomalous quartic gauge couplings in pp collisions at $\sqrt{s} = 7$ and 8 TeV

The CMS Collaboration*

Abstract

A search for exclusive or quasi-exclusive $\gamma\gamma \rightarrow W^+W^-$ production, via $pp \rightarrow p^{(*)}W^+W^-p^{(*)} \rightarrow p^{(*)}\mu^\pm e^\mp p^{(*)}$ at $\sqrt{s} = 8$ TeV, is reported using data corresponding to an integrated luminosity of 19.7 fb^{-1} . Events are selected by requiring the presence of an electron-muon pair with large transverse momentum $p_T(\mu^\pm e^\mp) > 30 \text{ GeV}$, and no associated charged particles detected from the same vertex. The 8 TeV results are combined with the previous 7 TeV results (obtained for 5.05 fb^{-1} of data). In the signal region, 13 (2) events are observed over an expected background of 3.9 ± 0.6 (0.84 ± 0.15) events for 8 (7) TeV, resulting in a combined excess of 3.4σ over the background-only hypothesis. The observed yields and kinematic distributions are compatible with the standard model prediction for exclusive and quasi-exclusive $\gamma\gamma \rightarrow W^+W^-$ production. Upper limits on the anomalous quartic gauge coupling operators $a_{0,C}^W$ (dimension-6) and $f_{M0,1,2,3}$ (dimension-8), the most stringent to date, are derived from the measured dilepton transverse momentum spectrum.

Published in the Journal of High Energy Physics as doi:10.1007/JHEP08(2016)119.

1 Introduction

A nonnegligible fraction of proton-proton collisions at the CERN LHC involves (quasi-real) photon interactions that provide a unique opportunity to study high-energy $\gamma\gamma$ processes at center-of-mass energies and integrated luminosities much higher than previously available [1]. Using the $\sqrt{s} = 7$ TeV data collected during Run 1 of the LHC, where Run 1 refers to the LHC data collection period between 2010-2012, measurements of $\gamma\gamma \rightarrow \mu^+\mu^-$ [2, 3] and $\gamma\gamma \rightarrow e^+e^-$ [3, 4] production were performed, followed by the first studies of $\gamma\gamma \rightarrow W^+W^-$ [5]. The latter process, occurring at leading order via the diagrams shown in Fig. 1, is particularly well suited to search for physics beyond the standard model (SM). Such deviations from the SM may be quantified through anomalous quartic gauge couplings (AQGC) of operators of dimension-6 or -8 [6, 7]. Specific models including anomalous gauge-Higgs couplings [8, 9], as well as composite Higgs [9–11] or warped extra dimensions [10] scenarios, will also result in deviations from the SM predictions for the $\gamma\gamma \rightarrow W^+W^-$ (differential and/or integrated) cross sections. Prior to the LHC, limits on AQGC were obtained through triboson ($Z\gamma\gamma$ and $W^+W^-\gamma$) production, and $WW \rightarrow \gamma\gamma$ scattering at LEP [12–18], and through $\gamma\gamma \rightarrow W^+W^-$ scattering at the Tevatron [19]. Anomalous quartic gauge couplings have been explored at the LHC through triboson ($W\gamma\gamma$ or $WV\gamma$, where V is a W or Z boson) production [20, 21], and same-charge $WW \rightarrow WW$ scattering [22, 23].

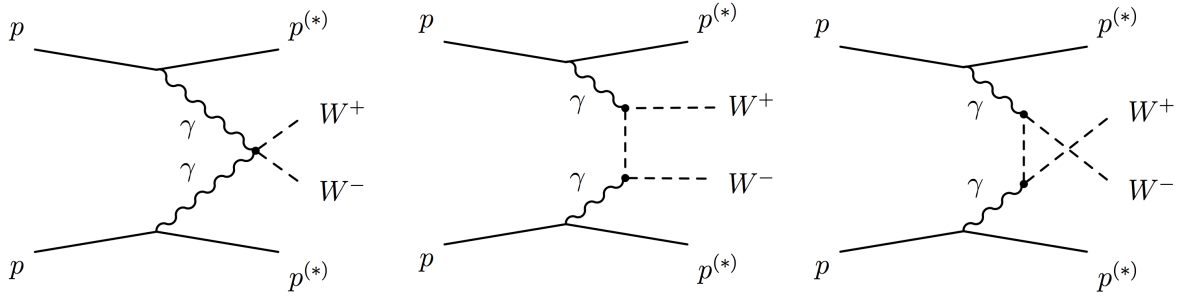


Figure 1: Quartic (left), t -channel (center), and u -channel (right) diagrams contributing to the $\gamma\gamma \rightarrow W^+W^-$ process at leading order in the SM. The $p^{(*)}$ indicates that the final state proton(s) remain intact (“exclusive” or “elastic” production), or dissociate (“quasi-exclusive” production).

This paper presents an update of the 7 TeV CMS $\gamma\gamma \rightarrow W^+W^-$ measurement [5], largely following the same analysis strategy as for 7 TeV but using the 8 TeV data set collected in 2012. The signal topology considered is $pp \rightarrow p^{(*)}W^+W^-p^{(*)}$, where the $p^{(*)}$ indicates that the final state protons either remain intact (“exclusive” or “elastic” production), or dissociate into an undetected system (“quasi-exclusive” or “proton dissociation” production). The $W^+W^- \rightarrow \mu^\pm e^\mp$ (plus undetected neutrinos) channel is the final state used to search for a signal, as the backgrounds due to Drell–Yan (DY) and $\gamma\gamma \rightarrow \ell^+\ell^-$ production are smaller than in the same-flavor final states. Events in which one or both of the W bosons decay into a tau lepton, with a subsequent decay of the tau to a muon or electron and neutrinos, are also included in the signal. In contrast to exclusive production, inclusive W^+W^- production is always accompanied by underlying event activity originating from semihard multiple-parton interactions and from softer “spectator” partons at forward rapidities. This will almost always result in the production of additional detectable charged particles from the $\mu^\pm e^\mp$ vertex. The experimental signature for the signal therefore consists of a muon-electron pair with large transverse momentum $p_T(\mu^\pm e^\mp)$, the vector p_T sum of the pair, originating from a common primary vertex with no additional charged particles detected.

Control samples of $\gamma\gamma \rightarrow \mu^+\mu^-$ and $\gamma\gamma \rightarrow e^+e^-$ events are used to study the efficiency of the exclusive selection in data, as well as the “rescattering” corrections [24, 25], from additional parton interactions between the protons, in quasi-exclusive collisions. Control regions in the dilepton p_T and charged-particle multiplicity distributions are used to study the main background contributions to the signal. Finally the $p_T(\mu^\pm e^\mp)$ distribution is used as the discriminating variable to measure the standard model $\gamma\gamma \rightarrow W^+W^-$ cross section, and to search for evidence of AQGC.

Sections 2–3 give a general description of the theory and the CMS detector, while Sections 4–5 describe the data sets, Monte Carlo (MC) simulations, and event selection. Sections 6–8 explain the 8 TeV analysis, and Section 9 describes the present 8 TeV results, as well as their combination with those from the previous 7 TeV study.

2 Phenomenology of anomalous couplings in $\gamma\gamma \rightarrow W^+W^-$ interactions

Within the SM, the triple ($WW\gamma$) and quartic ($WW\gamma\gamma$) couplings that contribute to $\gamma\gamma \rightarrow W^+W^-$ production are fully connected through the requirement of gauge invariance. In contrast, effective field theories can be constructed to quantify potential deviations from the SM by introducing genuine AQGCs through dimension-6 operators that are not related to the SM triple or quartic couplings [26]. By imposing $U(1)_{EM}$ and global custodial $SU(2)_C$ symmetries, and further requiring charge-conjugation and parity to be separately conserved, two such operators are allowed with couplings denoted a_0^W/Λ^2 and a_C^W/Λ^2 , where Λ is the energy scale for new physics. This approach corresponds to assuming a nonlinear representation of the spontaneously broken $SU(2) \otimes U(1)$ symmetry.

With the discovery of a light Higgs boson [27–29], a linear realization of the $SU(2) \otimes U(1)$ symmetry of the SM, spontaneously broken by the Higgs mechanism, is possible. Thus, the lowest order operators, where new physics may cause deviations in the quartic gauge boson couplings alone, are of dimension 8. In the dimension-8 formalism [30–32] there are fourteen operators contributing to $WW\gamma\gamma$ couplings, which in general will also generate a $WWZ\gamma$ vertex. By assuming that the anomalous $WWZ\gamma$ vertex vanishes, a direct relationship between the dimension-8 $f_{M,0,1,2,3}/\Lambda^4$ couplings and the dimension-6 $a_{0,C}^W/\Lambda^2$ couplings can be recovered [20, 30–32]:

$$\begin{aligned} \frac{a_0^W}{\Lambda^2} &= -\frac{4M_W^2}{e^2} \frac{f_{M,0}}{\Lambda^4}, \\ \frac{a_C^W}{\Lambda^2} &= \frac{4M_W^2}{e^2} \frac{f_{M,1}}{\Lambda^4}, \end{aligned} \tag{1}$$

where M_W is the mass of the W boson and e is the unit of electric charge. The $f_{M,2,3}/\Lambda^4$ couplings can be determined from the relations $f_{M,0} = 2f_{M,2}$ and $f_{M,1} = 2f_{M,3}$, which are a result of the constraint on the $WWZ\gamma$ vertex vanishing.

In both dimension-6 and dimension-8 scenarios, the $\gamma\gamma \rightarrow W^+W^-$ cross section in the presence of anomalous couplings would increase rapidly with the photon-photon center-of-mass energy $W_{\gamma\gamma}$. For couplings of the size that can be probed with the current data set, this would result in violation of unitarity at scales well below those reached in 7 and 8 TeV pp collisions at the LHC. To prevent this, various approaches modifying the effective Lagrangian have been proposed [33–35]. In this analysis, following the previous $\gamma\gamma \rightarrow W^+W^-$ results from the LHC

and Tevatron, we consider a dipole form factor with a cutoff scale Λ_{cutoff} :

$$a_{0,C}^W(W_{\gamma\gamma}^2) = \frac{a_{0,C}^W}{\left(1 + \frac{W_{\gamma\gamma}^2}{\Lambda_{\text{cutoff}}^2}\right)^2}.$$

We quote both the limits which preserve unitarity, with a dipole form factor and $\Lambda_{\text{cutoff}} = 500 \text{ GeV}$ as was used in previous publications [5, 19], and limits with $\Lambda_{\text{cutoff}} \rightarrow \infty$, which is equivalent to no form factor, violating unitarity.

The presence of anomalous couplings among the gauge bosons is expected to result in a harder spectrum of the transverse momentum of the W -pair system which can be probed experimentally by the hardness of the spectra in their decay products and, suitably, by that of the dilepton system of electron and muon.

3 The CMS detector

A detailed description of the CMS experiment can be found in Ref. [36]. The central feature of the CMS apparatus is a superconducting solenoid, of 6 m internal diameter. Within the field volume are the silicon pixel and strip tracker, the crystal electromagnetic calorimeter (ECAL) and the brass-scintillator hadronic calorimeter (HCAL). Muons are measured in gas-ionization detectors embedded in the steel flux-return yoke of the solenoid. The momentum resolution for electrons with $p_T \sim 45 \text{ GeV}$ from $Z \rightarrow ee$ decays ranges from 1.7% for nonshowering electrons in the barrel region to 4.5% for showering electrons in the endcaps [37]. The calorimeter cells are grouped in projective towers, of granularity $\Delta\eta \times \Delta\phi = 0.087 \times 0.087$ (where ϕ is the azimuthal angle in radians) in the pseudorapidity region $|\eta| < 1.5$, and increasing to 0.175×0.175 in the region $3 < |\eta| < 5$. The silicon tracker covers a range of $|\eta| < 2.4$, and consists of three layers made of 66 million $100 \times 150 \mu\text{m}^2$ pixels followed by ten microstrip layers, with strips of pitch between 80 and $180 \mu\text{m}$. The silicon tracker is used to detect charged particles as tracks. Muons are measured in the window $|\eta| < 2.4$, with detection planes made of three technologies: drift tubes, cathode strip chambers, and resistive-plate chambers. Thanks to the strong magnetic field, 3.8 T, and to the high granularity of the silicon tracker, the transverse momentum, p_T , of the muons matched to silicon tracks is measured with a resolution better than 1.5%, for p_T smaller than 100 GeV. The resolution of z_0 , the point of closest approach of the track to the beam direction z , for a 1 (10) GeV pion is 100–300 μm (30–60 μm) in the central region and 300–1000 μm (60–150 μm) in the forward region [38]. The ECAL provides coverage in a range of $|\eta| < 1.48$ in a barrel region, and $1.48 < |\eta| < 3$ in two endcap regions (EE). A preshower detector consisting of two planes of silicon sensors interleaved with a total of 3 radiation lengths of lead is located in front of the EE. The first level of the CMS trigger system, composed of custom hardware processors, uses information from the calorimeters and muon detectors to select (in less than 4 μs) the most interesting events. The high-level trigger processor farm further decreases the event rate from 100 kHz to a few hundred Hz, before data storage.

4 Data sets and Monte Carlo simulation

The analyzed data samples consist of 19.7 fb^{-1} of proton-proton collisions collected in 2012 at a center-of-mass energy of $\sqrt{s} = 8 \text{ TeV}$. This measurement is combined with a similar analysis carried out in 2011 using 5.05 fb^{-1} of pp collisions collected at a center-of-mass energy of $\sqrt{s} = 7 \text{ TeV}$. During Run 1 of the LHC the number of overlapping interactions per bunch crossing

(“pileup”) was nonnegligible. In the 8 (7) TeV data-taking period the average pileup was 21 (9) interactions per crossing. The 7 TeV data analysis is described in Ref. [5], and the rest of this section focuses on describing the 8 TeV data analysis.

The simulated SM and anomalous signal samples of $\gamma\gamma \rightarrow W^+W^-$ are generated with MADGRAPH [39, 40] v5 release 2.0.0, using the equivalent photon approximation (EPA) [41]. Cross-checks with CALCHEP [42] v3.4 have also been performed since this is the generator used for simulated SM and anomalous signal samples for the 7 TeV analysis. The elastic and proton dissociation $\gamma\gamma \rightarrow \ell^+\ell^-$ samples are produced using the LPAIR v4.0 generator [43, 44].

The backgrounds from inclusive diboson, W +jets, and $t\bar{t}$ production are simulated with MADGRAPH. For $t\bar{t}$ production the yields are normalized to the next-to-next-to-leading-order (NNLO) plus next-to-next-to-leading-logarithmic cross section prediction obtained with Top++2.0 [45]. For inclusive diboson and W +jets production the yields are normalized to the NNLO and next-to-leading-order cross section predictions, respectively, and are obtained with MCFM v6.6 [46]. Inclusive Drell–Yan samples are simulated with POWHEG v1.0 [47–49]. The outgoing partons from the matrix element calculation in both MADGRAPH and POWHEG are matched to parton showers from the PYTHIA v6.4.26 [50] with the Z2* tune [51] for the analysis of the 8 TeV data and with the Z2 tune [52] for the analysis of the 7 TeV data. The simulated inclusive W^+W^- sample does not include events generated in diffractive topologies, in which one of the incoming protons remains intact. While diffractive W^+W^- production is expected to be small compared to the rate of inclusive W^+W^- production, the mean multiplicity of charged particles in diffractive events will be smaller, thus enhancing the contribution of diffractive production to the exclusive signal region. The contribution from diffractive W^+W^- production is simulated with POMPYT v2.6.1 [53], using diffractive parton distribution functions obtained from the H1 fit B to diffractive deep inelastic scattering data [54]. In practice, the diffractive W^+W^- background may be suppressed by a “gap survival probability” factor, representing the effect of rescattering interactions that will lead to additional hadronic activity in the event. As this factor is not precisely predicted or measured at LHC energies [55], a very conservative 100% gap survival probability (meaning no correction due to rescattering interactions) is assumed. Gluon-induced central exclusive production of W^+W^- pairs, with an additional “screening” gluon emission to cancel the color flow, is expected to be heavily suppressed [56] and is neglected in the current analysis.

Electroweak production (at order α_{EW}^5 or α_{EW}^6 for real W^+W^- emission) of W^+W^- pairs, including $WW \rightarrow WW$ scattering, is also not included in the simulated inclusive W^+W^- sample. We use a sample generated with MADGRAPH, which describes well the electroweak production of $Zq\bar{q}$ (where ‘q’ indicates a quark jet) at $\sqrt{s} = 8$ TeV [57], to estimate the central value of the electroweak $W^+W^-q\bar{q}$ background, with PHANTOM v1.0 [58] used for systematic studies.

All simulated samples are passed through a detailed GEANT4 simulation [59] of the CMS detector. The same algorithms are used to reconstruct both the simulated samples and collision data.

5 Event selection

The event selection is similar for both $\mu^\pm e^\mp$ final states used to search for a W^+W^- signal, and for the $\mu^+\mu^-$ and e^+e^- final states used as control samples. The events are triggered by the presence of two leptons with transverse momentum $p_T > 17(8)$ GeV for the leading (subleading) lepton.

Offline, the leptons are required to be of opposite charge, to have $p_T > 20$ GeV, to pass “tight” identification criteria for muons [60] and “medium” identification criteria for electrons [37], and come from the same reconstructed primary vertex. Primary vertices are identified by clustering tracks according to a deterministic annealing algorithm, and subsequently performing a fit to the clustered tracks [38]. The “tight” muon identification includes requirements on the minimum number of muon detector planes hit, the minimum number of hits in the pixel detector and of layers hit in the silicon strip detector, the goodness of the global fit to the muon track, and the transverse impact parameter with respect to the primary vertex. An additional requirement that the longitudinal impact parameter be at most 5 mm is added for the 8 TeV analysis and was not present in the 7 TeV analysis. This requirement is added to suppress cosmic muons, muons from decays in flight of charged mesons, and tracks from pileup. The “medium” identification criteria for electrons combines information from the ECAL, HCAL, and silicon tracker. This includes selections on the azimuthal angle and pseudorapidity differences between the tracks and ECAL deposits associated to the electron candidate, the ratio of energy deposited in the HCAL to that in the ECAL, the shower shape of the ECAL deposits, and the compatibility of the energy deposited in the ECAL with the momentum of the associated track. The efficiency of the “tight” muon identification is estimated to be $\geq 96\%$ for muons with $p_T > 20$ GeV, with a hadron misidentification probability of $< 0.5\%$. The efficiency of the “medium” electron identification rises from $\sim 60\%$ for electrons with $p_T = 20$ GeV, reaching a plateau at $\geq 80\%$ for electrons with $p_T > 55$ GeV. The misidentification probability is estimated to be $< 4\%$ for the “medium” electron identification. In addition, the electrons are required to satisfy relative isolation criteria, based on the global particle-flow algorithm [61, 62]. The invariant dilepton mass is also required to satisfy $m(\ell^+\ell^-) > 20$ GeV in order to remove any potential background due to low-mass resonances, which is particularly relevant in the $\mu^+\mu^-$ and e^+e^- final states.

The final signal region is then defined by the presence of an opposite-charge electron-muon pair originating from a common primary vertex that has no additional tracks associated with it, and has transverse momentum $p_T(\mu^\pm e^\mp) > 30$ GeV. The zero-additional-tracks requirement is motivated by the lack of underlying event activity expected for exclusive and quasi-exclusive $\gamma\gamma \rightarrow W^+W^-$ production, in which the beam protons remain intact or dissociate into an undetected forward system respectively, in contrast to backgrounds from inclusive diboson production. The $p_T(\mu^\pm e^\mp) > 30$ GeV requirement is designed to suppress backgrounds from $\tau^+\tau^-$ production, including the exclusive and quasi-exclusive $\gamma\gamma \rightarrow \tau^+\tau^-$ processes.

6 The $\gamma\gamma \rightarrow \ell^+\ell^-$ control samples and corrections

In the $\mu^+\mu^-$ and e^+e^- final states, backgrounds due to direct $\gamma\gamma \rightarrow \ell^+\ell^-$ production and Drell-Yan processes are much larger than in the $\mu^\pm e^\mp$ channel. Therefore these channels are used as control samples to study both the efficiency of the zero-additional-tracks selection, and the theoretically poorly known proton dissociation contribution to high-mass $\gamma\gamma$ interactions [63].

6.1 Efficiency correction for track veto

First, in order to select a high-purity sample of elastic $pp \rightarrow p\ell^+\ell^-p$ events and study the efficiency of the additional track veto, we apply harsh selection criteria to the kinematics of the lepton pair. These consist in requiring a small acoplanarity, $|1 - \Delta\phi(\ell^+\ell^-)/\pi| < 0.01$ where $\Delta\phi(\ell^+\ell^-)$ is the difference in azimuthal angle between the two leptons, and an invariant mass incompatible with $Z \rightarrow \ell^+\ell^-$ decays ($m(\ell^+\ell^-) < 70$ GeV or $m(\ell^+\ell^-) > 106$ GeV). The leptons from elastic $pp \rightarrow p\ell^+\ell^-p$ events have small acoplanarity because the very small virtuality of

the exchanged photons results in a dilepton pair produced with $p_T(\ell^+\ell^-) \sim 0$. The acoplanarity and invariant mass requirements result in a sample expected to contain a negligible contribution from inclusive backgrounds, but some contamination from $\gamma\gamma \rightarrow \ell^+\ell^-$ events where one or both of the protons dissociate. In this control sample we find a deficit in the data compared to the theoretical prediction for events with zero additional tracks associated to the dilepton vertex (Fig. 2). We have verified that this is due to the fact that the efficiency of the additional-track veto is overestimated in the simulation. To numerically calculate the data-to-simulation ratio, we use a tighter acoplanarity requirement ($|1 - \Delta\phi(\ell^+\ell^-)/\pi| < 0.001$, corresponding to $>3\sigma$ in terms of the experimental resolution on the acoplanarity) to further reduce the contamination from $\gamma\gamma \rightarrow \ell^+\ell^-$ events where one or both of the protons dissociate. The data-to-simulation ratio is 0.63 ± 0.04 in the $\mu^+\mu^-$ channel and 0.63 ± 0.07 in the e^+e^- channel. By comparing the shapes of the $\gamma\gamma \rightarrow \ell^+\ell^-$ distributions we find a good data-to-theory agreement, apart from the overall difference in normalization (Figs. 2 and 3). We therefore apply this ratio, averaged over the $\mu^+\mu^-$ and e^+e^- samples, as a track veto efficiency correction to the $\gamma\gamma \rightarrow W^+W^-$ signal.

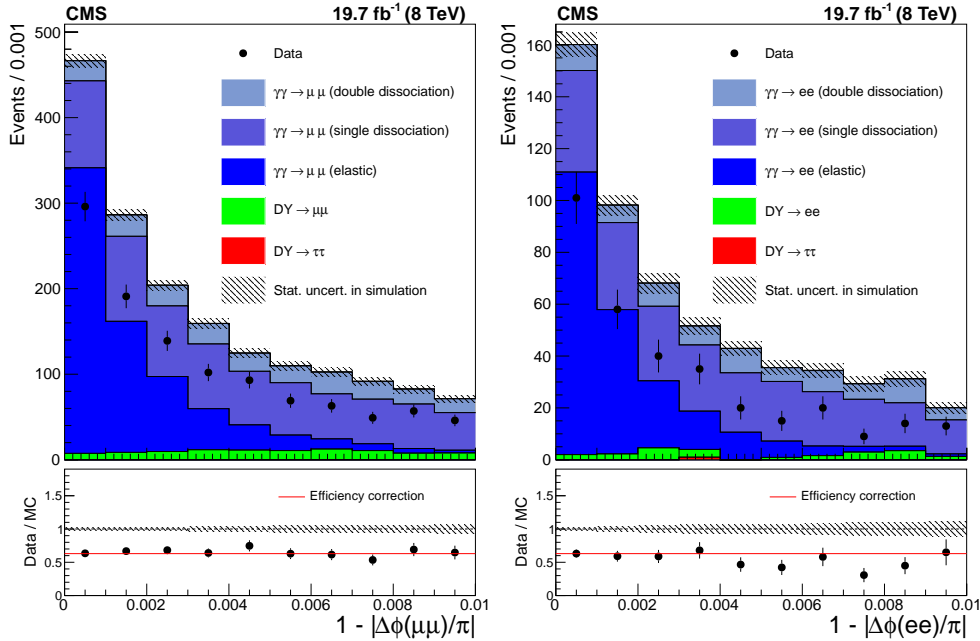


Figure 2: Acoplanarity for the $\mu^+\mu^-$ (left) and e^+e^- (right) final states in the elastic $\gamma\gamma \rightarrow \ell^+\ell^-$ control region ($|1 - \Delta\phi(\ell^+\ell^-)/\pi| < 0.01$ and $m(\ell^+\ell^-) < 70$ GeV or $m(\ell^+\ell^-) > 106$ GeV) and 0 additional tracks associated to the dilepton vertex. The data (points with error bars) are compared to the simulated samples (histograms) in the top panels. The data/MC ratios are shown in the bottom panels (the red line shows the extracted correction for the track veto efficiency).

In exclusive and quasi-exclusive production, additional tracks identified as coming from the dilepton vertex are predominantly misassociated tracks originating from other pileup vertices in the event. These are mainly very low- p_T , forward tracks not modeled perfectly by the simulation. Therefore a track veto efficiency correction is applied to account for the resulting migration of signal events to higher multiplicities. For inclusive backgrounds, migrations may happen in both directions, with tracks from pileup vertices being wrongly associated with a dilepton vertex, or tracks from the underlying event being wrongly associated with a pileup vertex. For the largest background of inclusive W^+W^- production, the simulation is observed to reproduce the data in the relevant control region; therefore no correction is applied to the

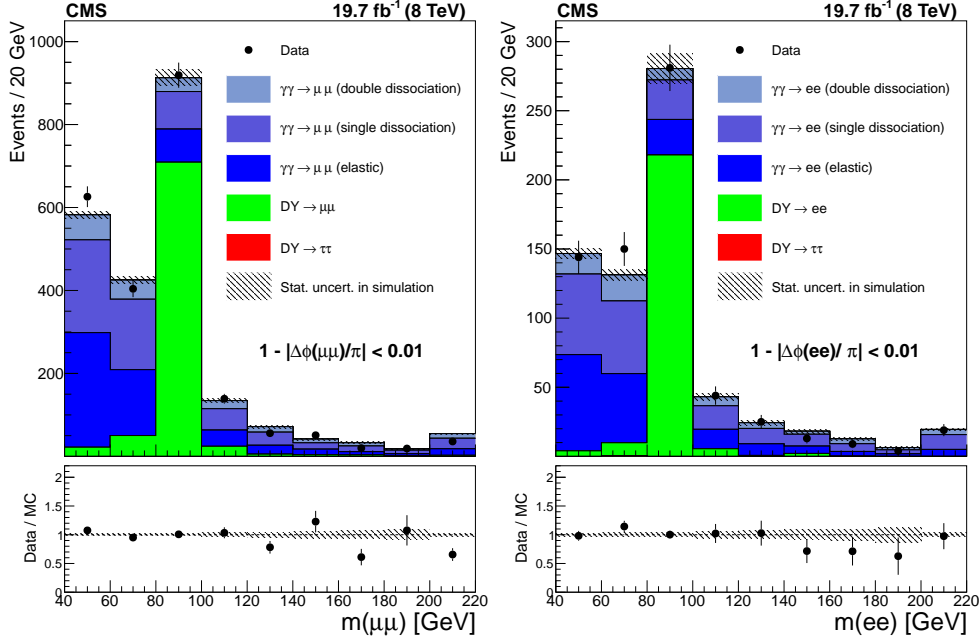


Figure 3: Dilepton invariant mass for the $\mu^+\mu^-$ (left) and e^+e^- (right) final states with an acoplanarity requirement, $|1 - \Delta\phi(\ell^+\ell^-)/\pi| < 0.01$, and zero additional tracks associated to the dilepton vertex. The data (points with error bars) are compared to the simulated samples (histograms) in the top panels, and the data/MC ratios are shown in the bottom panels. The exclusive-production simulated samples are scaled to the number of events in data for $m(\ell^+\ell^-) < 70$ GeV or $m(\ell^+\ell^-) > 106$ GeV. The Drell–Yan simulation is scaled to the number of events in data for $70 < m(\ell^+\ell^-) < 106$ GeV. The last bin in both plots is an overflow bin and includes all events with invariant mass greater than 200 GeV.

backgrounds.

6.2 Proton dissociation contribution

Simulations of high-mass $\gamma\gamma$ interactions with the LPAIR matrix element generator show that they predominantly occur in events where at least one of the protons dissociates. However, the cross section calculations do not include rescattering effects, in which additional gluon interactions between the protons produce extra hadronic activity in the event besides the final-state leptons or gauge bosons. As a result of these rescattering corrections, $\gamma\gamma \rightarrow \ell^+\ell^-$ and $\gamma\gamma \rightarrow W^+W^-$ signal events will migrate to higher multiplicities. This is expected to be a large effect, particularly for events in which both protons dissociate, with up to about 90% of events being nonexclusive, depending on the exact kinematic range studied [25, 63]. The contribution from proton dissociation is therefore estimated directly from the data, rather than relying on simulation.

To estimate the contribution due to proton dissociation in a kinematic region similar to the W^+W^- signal, we select a sample of dilepton events with invariant mass greater than 160 GeV, corresponding to the threshold for the production of two on-shell W bosons, with no additional tracks associated with the dilepton vertex. We then compute the ratio of the number of events measured in this region to the predicted number of elastic $pp \rightarrow p\ell^+\ell^-p$ events, with the additional track veto efficiency correction applied and the Drell–Yan contribution subtracted from the data. This results in a scale factor $F = 4.10 \pm 0.43$, with the uncertainty determined from the statistical uncertainty of the data control sample, that is used to correct the elastic

$pp \rightarrow pW^+W^-p$ prediction to the total $pp \rightarrow p^{(*)}W^+W^-p^{(*)}$ prediction, including proton dissociation.

Figure 4 shows the dilepton invariant mass distribution for events with no additional tracks at the dilepton vertex. The theoretical double-dissociation contribution (blue dotted line on top of the sum of all other simulated data samples in Fig. 4) is much larger than the data, because the value of the gap survival probability factor is too high in the calculations, whereas at high dilepton mass the data are consistent with a very low survival probability for this contribution. For a 100% gap survival probability in both single- and double-dissociation processes, the scale factor to correct the elastic prediction would be $F = 7.71 \pm 0.57$, by applying the same procedure described above but using the single- and double-dissociation simulated samples. However, if the double-dissociation contribution is assumed to have a gap survival probability of 0% (maximum predicted rescattering), whereas the single-dissociation contribution is assumed to have a gap survival probability of 100% (no rescattering), the proton dissociation factor estimated from the simulation would be $F = 4.39 \pm 0.48$. This factor is compatible with that extracted from the data-driven method described above and is also consistent with the expectation from theory [25, 64] that the single-dissociation contribution has a large gap survival probability while the double-dissociation contribution has a small gap survival probability.

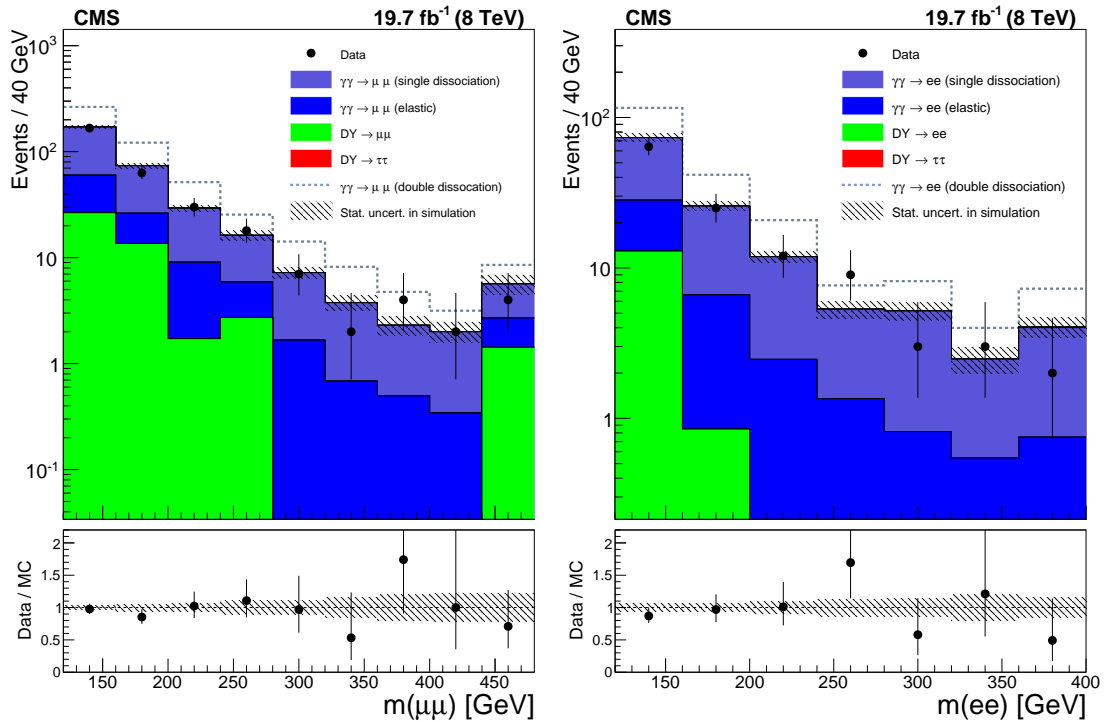


Figure 4: Dilepton invariant mass for the $\mu^+\mu^-$ (left) and e^+e^- (right) final states in the $\gamma\gamma \rightarrow \ell^+\ell^-$ proton dissociation control region with no additional tracks associated to the dilepton vertex, for data (points with error bars) and simulated samples (histograms, with the efficiency correction applied to the exclusive samples). The last bin in both plots is an overflow bin and includes all events above the maximum value in the plot. The bottom panels show the data/MC ratio where the denominator includes the sum of all simulated samples except the double-dissociation contribution (shown as the blue dotted line in the top plots).

7 Backgrounds

7.1 Inclusive diboson backgrounds

The dominant inclusive diboson backgrounds consist mainly of W^+W^- events, with a small contribution from WZ and ZZ events. As indicated in Table 1, the inclusive diboson background is reduced by a factor of more than 300 by vetoing on additional tracks at the $\mu^\pm e^\mp$ vertex. The remaining backgrounds are studied by selecting electron-muon vertices with $p_T(\mu^\pm e^\mp) > 30$ GeV, and 1–6 additional tracks. The event yields and kinematic distributions are compatible with the expectations from simulation, with 247.0 ± 8.0 (stat) events expected and 214 events observed in data (Fig. 5).

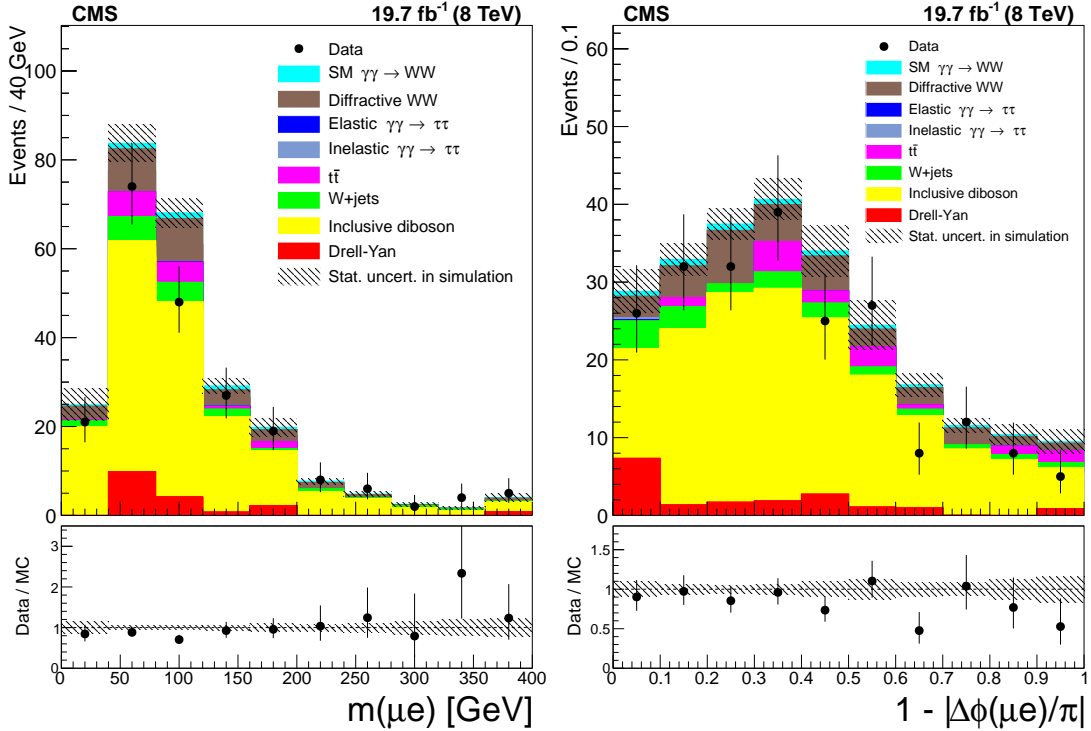


Figure 5: Distributions of $\mu^\pm e^\mp$ invariant mass (left) and acoplanarity (right) for data (points with error bars) and expected backgrounds (histograms) for $p_T(\mu^\pm e^\mp) > 30$ GeV and 1–6 extra tracks (inclusive W^+W^- control region). The last bin in the invariant mass plot is an overflow bin and includes all events with $m(\mu e) > 360$ GeV. The bottom panels show the data/MC ratio.

The inclusive W^+W^- background estimate obtained using MADGRAPH for the signal region (no additional tracks and $p_T(\mu^\pm e^\mp) > 30$ GeV) is 2.2 ± 0.4 (stat) events. The prediction is additionally cross-checked with an estimate based on PYTHIA, which also describes well the control region with 1–6 extra tracks. This results in an inclusive W^+W^- background prediction of 2.5 ± 0.9 (stat) events, consistent with the default prediction using MADGRAPH. The WZ and ZZ background estimates are obtained from MADGRAPH as well, and only contribute 0.1 ± 0.1 (stat) events in the signal region.

7.2 W+jets background

The background due to W +jets production, with one genuine lepton and one misidentified or nonprompt lepton in a jet, is expected to be small. To study this background in data, a control sample, expected to be dominated by W +jets, is selected with the $p_T(\mu^\pm e^\mp) > 30$ GeV

requirement, where at least one of the two leptons has failed the nominal offline identification described in Section 5. The control sample is expected to contain 78% W +jets events. To extract a prediction for the W +jets background contribution in which both leptons pass the nominal lepton identification requirements, we use the ratio of the number of events in the signal and control regions calculated from simulation and multiply this ratio by the number of data events in the control region. The resulting prediction in the signal region is 0.2 ± 0.1 (stat) events, approximately 5% of the total background.

7.3 Drell–Yan background

The background due to DY $\tau^+\tau^-$ production is suppressed by a factor of more than 700 by the requirement of no additional tracks associated with the $\mu^\pm e^\mp$ vertex (Table 1). To check the modeling of the DY background contribution, a control region with $p_T(\mu^\pm e^\mp) < 30$ GeV and 1–6 additional tracks is selected, resulting in a sample that is expected to contain 87% DY $\tau^+\tau^-$ events. We find an overall deficit in the data with respect to the prediction from simulation, with 771 events observed and 1008 ± 27 (stat) events expected. Figure 6 shows that this deficit appears at low mass and low-acoplanarity where the DY background is expected. At higher values of the mass and acoplanarity where the inclusive W^+W^- contribution is significant, the data agree well with the simulation, consistent with the behavior observed in the W^+W^- control region. The number of simulated DY events surviving in the signal region after all selections is zero, therefore no rescaling of the DY background is performed based on the control region yields.

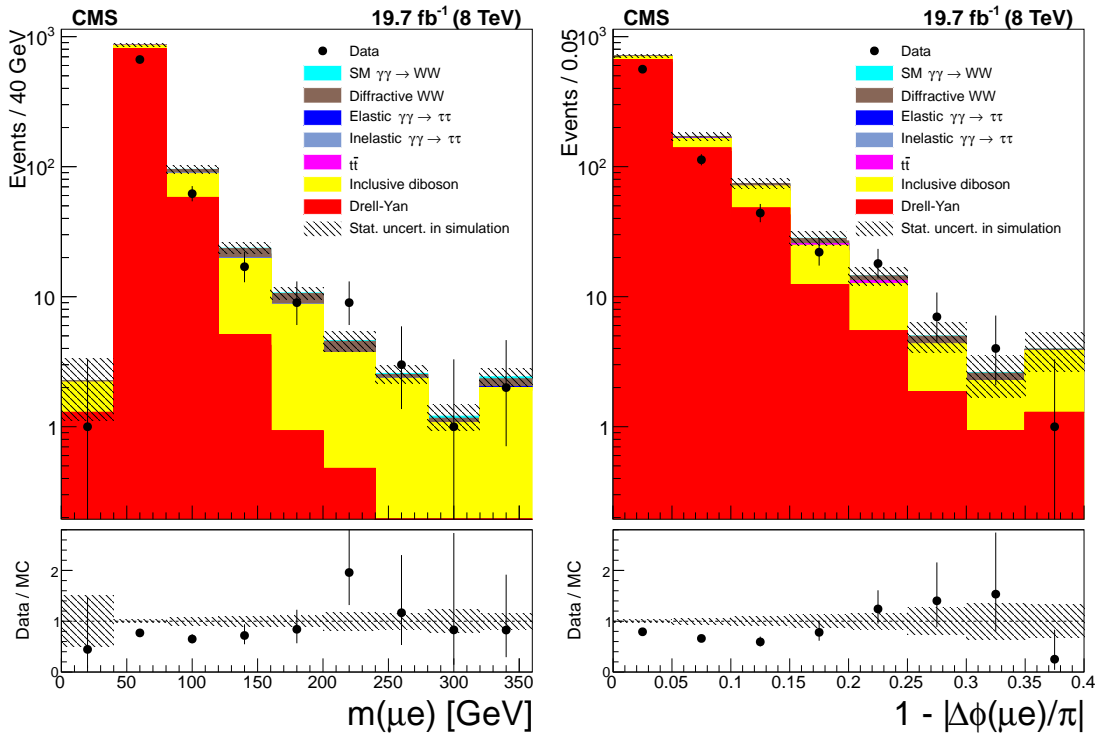


Figure 6: Distributions of $\mu^\pm e^\mp$ invariant mass (left) and acoplanarity (right) for data (points with error bars) and expected backgrounds (histograms) for $p_T(\mu^\pm e^\mp) < 30$ GeV and 1–6 extra tracks (Drell–Yan $\tau^+\tau^-$ control region). The last bin in both plots is an overflow bin and includes all events above the maximum value in the plot. The bottom panels show the data/MC ratio.

7.4 The $\gamma\gamma \rightarrow \tau^+\tau^-$ background

As $\gamma\gamma \rightarrow \tau^+\tau^-$ is produced in both exclusive and quasi-exclusive topologies, it cannot be completely eliminated by requiring no additional tracks at the $\mu^\pm e^\mp$ vertex. The requirement that $p_T(\mu^\pm e^\mp) > 30$ GeV, however, combined with the 20 GeV single-lepton thresholds, reduces this background to approximately one event in the signal region (Table 1).

A control sample enriched in $\gamma\gamma \rightarrow \tau^+\tau^-$ events is selected by requiring an electron-muon vertex with no additional associated tracks, and $p_T(\mu^\pm e^\mp) < 30$ GeV. In data, 11 events are observed, compared to a prediction of 12.9 ± 2.5 , including 3.4 ± 0.5 events expected from $\gamma\gamma \rightarrow \tau^+\tau^-$ production. The kinematic distributions are in good agreement with the predicted sum of $\gamma\gamma \rightarrow \tau^+\tau^-$ and other backgrounds (Fig. 7).

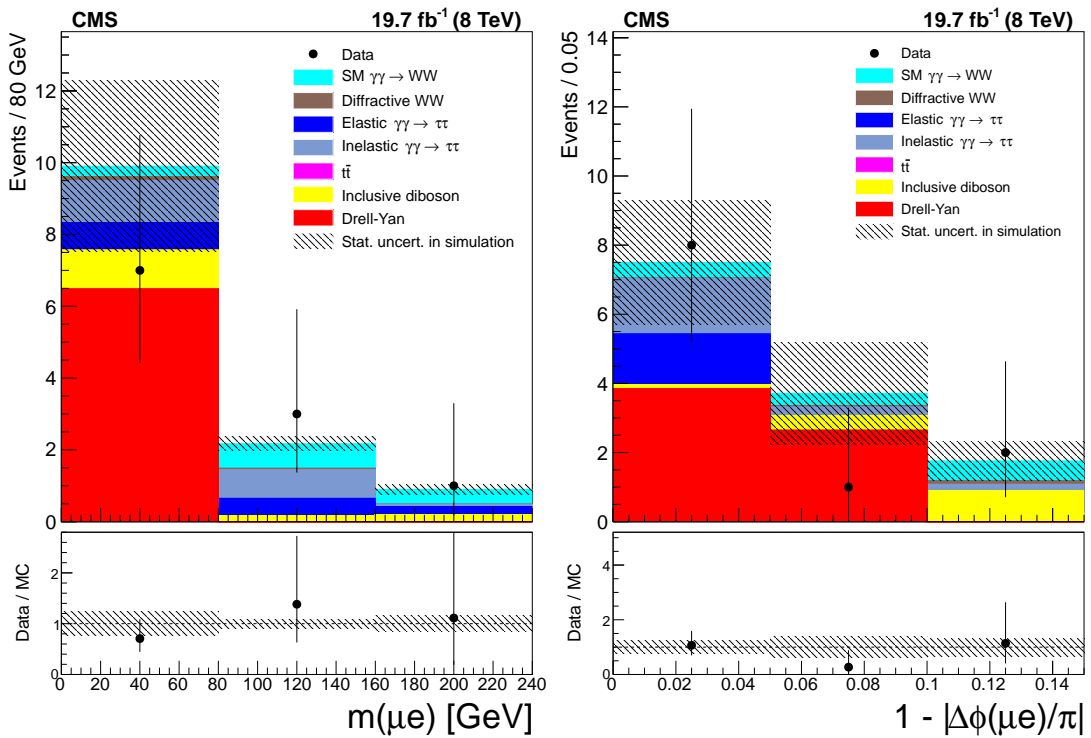


Figure 7: Distributions of $\mu^\pm e^\mp$ invariant mass (left) and acoplanarity (right) for data (points with error bars) and expected backgrounds (histograms) for $p_T(\mu^\pm e^\mp) < 30$ GeV and no additional tracks ($\gamma\gamma \rightarrow \tau^+\tau^-$ control region). The last bin in both plots is an overflow bin and includes all events above the maximum value in the plot. The bottom panels show the data/MC ratio.

7.5 Summary of backgrounds

The number of expected signal and background events at each stage of the selection is shown in Table 1. As described in Section 4, the diffractive W^+W^- background is estimated from simulation, assuming the maximal gap survival probability of 100%. By assuming a smaller survival probability the total background prediction would decrease by at most 0.1 events, which is less than 3% of the total background and less than 2% of the expected SM signal. The “Other backgrounds” category includes the contributions of $t\bar{t}$, W +jets, electroweak $W^+W^-q\bar{q}$, diffractive W^+W^- , and jets. The total expected background is 3.9 ± 0.6 events, with the largest contribution coming from inclusive W^+W^- production. The expected SM signal is 5.3 ± 0.7 events.

As a final check for potential mismodeled backgrounds, we examine same-charge $\mu^\pm e^\pm$ events. In the control region with 1–6 extra tracks and $p_T(\mu^\pm e^\pm) > 30 \text{ GeV}$, 28 such events are observed, with track multiplicity and invariant mass distributions consistent with the simulation, which predicts 20.6 ± 2.1 events. In the signal-like region with no additional tracks and $p_T(\mu^\pm e^\pm) > 30 \text{ GeV}$, no same-charge events are observed in the data, consistent with the prediction of 0.12 background events from simulation.

Table 1: Number of expected signal and background events in simulation passing each selection step, normalized to an integrated luminosity of 19.7 fb^{-1} . The preselection includes events with an opposite-charge muon and electron associated with the same vertex, each with $p_T > 20 \text{ GeV}$ and $|\eta| < 2.4$, and < 16 additional tracks at the vertex. Uncertainties are statistical only.

Selection step	Data	Exclusive $\gamma\gamma \rightarrow WW$	Total background	Inclusive diboson	Drell-Yan	$\gamma\gamma \rightarrow \tau\tau$	Other backgrounds
Trigger and Preselection	19406	26.9 ± 0.2	22180 ± 1890	1546 ± 15	7093 ± 75	18.1 ± 0.8	13520 ± 1890
$m(\mu^\pm e^\mp) > 20 \text{ GeV}$	18466	26.6 ± 0.2	21590 ± 1850	1507 ± 15	7065 ± 75	18.1 ± 0.8	13000 ± 1850
Muon and electron identification	6541	22.5 ± 0.2	6640 ± 93	1306 ± 11	4219 ± 58	12.6 ± 0.7	1102 ± 72
$\mu^\pm e^\mp$ vertex with no add. tracks	24	6.7 ± 0.2	15.2 ± 2.5	3.7 ± 0.7	6.5 ± 2.3	4.3 ± 0.5	0.7 ± 0.1
$p_T(\mu^\pm e^\mp) > 30 \text{ GeV}$	13	5.3 ± 0.1	3.9 ± 0.5	2.3 ± 0.4	0.1 ± 0.1	0.9 ± 0.2	0.6 ± 0.1

8 Systematic uncertainties

We consider systematic uncertainties related to the integrated luminosity, the lepton trigger and selection efficiency, the efficiency of the additional track veto, and the uncertainty in the proton dissociation contribution.

The integrated luminosity uncertainty for the 8 TeV data set used in this measurement is estimated to be 2.6% [65]. The trigger and lepton identification efficiencies are corrected for differences between data and simulation using control samples of $Z \rightarrow \ell^+ \ell^-$ events. The systematic uncertainty is estimated from the statistical uncertainty associated with the correction applied, resulting in an uncertainty of 2.4% in the signal efficiency.

The correction for the efficiency of the additional track veto is obtained from the control samples of elastic-enriched $\gamma\gamma \rightarrow \ell^+ \ell^-$ events, as described in Section 6. Since the correction factors obtained in the $\mu^+ \mu^-$ and $e^+ e^-$ channels are consistent, they are combined to obtain the final correction factor. The systematic uncertainty is estimated from the statistical uncertainty associated with the correction applied, resulting in an overall uncertainty of 5% in the signal efficiency.

The normalization factor for the proton dissociation contribution to the signal is obtained from high-mass $\gamma\gamma \rightarrow \ell^+ \ell^-$ events in data as explained in Section 6. The statistical uncertainty in this factor is 9.2%, based on the combination of the $\mu^+ \mu^-$ and $e^+ e^-$ channels. An additional effect of 5.0% must be included to describe the difference between the matrix element prediction of LPAIR used in the method described in Section 6, and the equivalent photon approximation used to generate signal events. Adding in quadrature these contributions results in an overall systematic uncertainty of 10.5% related to the proton dissociation contribution. It is also checked that the proton dissociation factor does not vary as a function of the dilepton invariant mass threshold, between 100–400 GeV.

The full list of systematic uncertainties for the signal efficiency is shown in Table 2. The overall systematic uncertainty assigned to the signal is 12.2%. The systematic uncertainties considered for the background prediction include the limited statistics of the relevant simulation or data control samples, integrated luminosity, trigger efficiency, and lepton identification efficiency.

In addition, an uncertainty of ± 0.24 events in the electroweak W^+W^- background contribution is included, corresponding to the difference between the background predictions of the MADGRAPH and PHANTOM generators.

Table 2: Summary of systematic uncertainties affecting the signal.

	Uncertainty
Proton dissociation factor	10.5%
Efficiency correction for no add. tracks	5.0%
Trigger and lepton identification	2.4%
Integrated luminosity	2.6%
Total	12.2%

9 Results

The total expected signal from standard model exclusive or quasi-exclusive $\gamma\gamma \rightarrow W^+W^-$ production in the 8 TeV data set is 5.3 ± 0.7 events, with an expected background of 3.9 ± 0.6 events. This corresponds to a mean expected signal significance of 2.1σ . Figure 8 shows the $p_T(\mu^\pm e^\mp)$ and extra-tracks multiplicity distributions for events passing all other selection requirements. In the signal region with no additional tracks and $p_T(\mu^\pm e^\mp) > 30$ GeV, 13 events are observed in the data that pass all the selection criteria. The properties of the selected events, including the $\mu^\pm e^\mp$ invariant mass, acoplanarity, and missing transverse energy (E_T^{miss}), are consistent with the SM signal plus background prediction (Fig. 9).

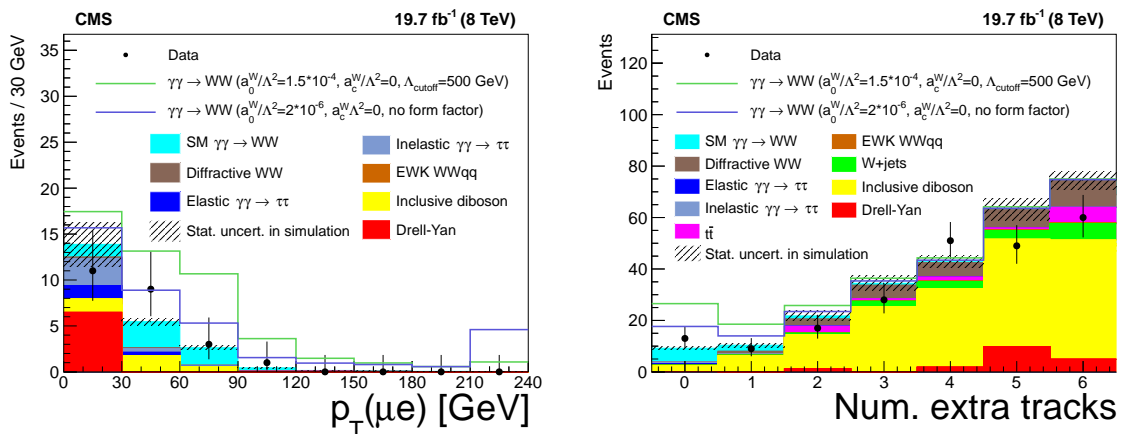


Figure 8: Distributions of muon-electron transverse momentum for events with zero associated tracks (left), and extra-tracks multiplicity for events with $p_T(\mu^\pm e^\mp) > 30$ GeV (right). The data are shown by the points with error bars; the histograms indicate the expected SM signal and backgrounds. Two representative values for anomalous couplings are shown stacked on top of the backgrounds. The last bin in the $p_T(\mu^\pm e^\mp)$ distribution is an overflow bin and includes all events with $p_T(\mu^\pm e^\mp) > 210$ GeV.

The observed significance above the background-only hypothesis in the 8 TeV data, including systematic uncertainties, is 3.2σ . In the 7 TeV data, two events were observed in the signal region, with an expected background of 0.84 ± 0.15 events, corresponding to an observed (expected) significance of 0.8σ (1.8σ). We combine the 7 and 8 TeV results, treating all systematic uncertainties as fully uncorrelated between the two measurements, with the exception of the 5% uncertainty from the use of the equivalent photon approximation in the generation of signal

samples, which is treated as fully correlated between the two analyses. The resulting observed (expected) significance for the 7 and 8 TeV combination is 3.4σ (2.8σ), constituting evidence for $\gamma\gamma \rightarrow W^+W^-$ production in proton-proton collisions at the LHC.

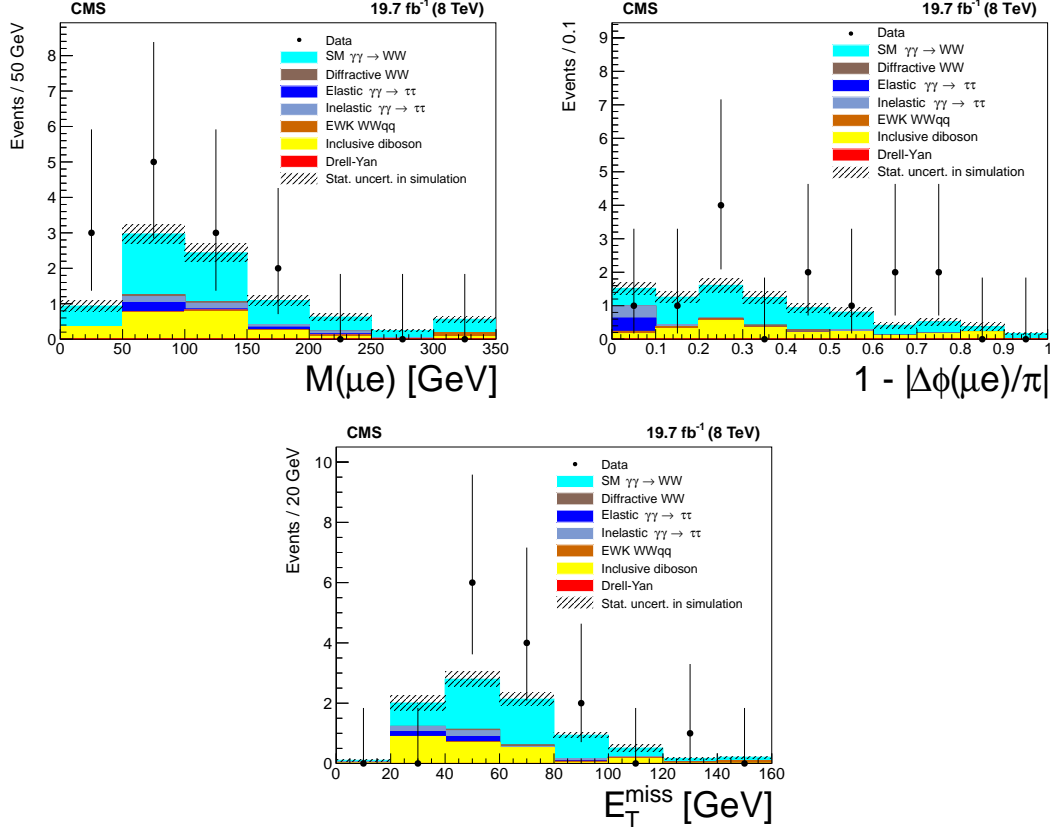


Figure 9: Muon-electron invariant mass (top left), acoplanarity (top right), and missing transverse energy (bottom) in the $\gamma\gamma \rightarrow W^+W^-$ signal region. The data are shown by the points with error bars; the histograms indicate the expected SM signal and backgrounds. The last bin in the invariant mass and missing transverse energy plots is an overflow bin and includes also all events above the maximum value in the plot.

9.1 Cross section measurement

Interpreting the 8 TeV results as a cross section multiplied by the branching fraction to $\mu^\pm e^\mp$ final states, corrected for all experimental efficiencies and extrapolated to the full phase space, yields:

$$\sigma(pp \rightarrow p^{(*)}W^+W^-p^{(*)} \rightarrow p^{(*)}\mu^\pm e^\mp p^{(*)}) = 10.8_{-4.1}^{+5.1} \text{ fb.}$$

The SM prediction is 6.2 ± 0.5 fb, with the elastic component calculated with MADGRAPH and then rescaled by the proton dissociation factor. The uncertainty on the SM prediction reflects the uncertainty in the proton dissociation contribution to the signal. The acceptance for the SM signal calculated from the simulation is $57.8 \pm 0.9\%$.

The corresponding 95% confidence level (CL) upper limit obtained from the 7 TeV data was [5]:

$$\sigma(pp \rightarrow p^{(*)}W^+W^-p^{(*)} \rightarrow p^{(*)}\mu^\pm e^\mp p^{(*)}) < 10.6 \text{ fb,}$$

with a central value of $2.2_{-2.0}^{+3.3}$ fb. The corresponding SM prediction at 7 TeV is 4.0 ± 0.7 fb, with the uncertainty reflecting that of the proton dissociation contribution to the signal.

9.2 Anomalous couplings

We use the dilepton transverse momentum $p_T(\mu^\pm e^\mp)$ (Fig. 8, left) as a discriminating variable to extract limits on AQGCs. Two bins, with boundaries $p_T(\mu^\pm e^\mp) = 30\text{--}130\text{ GeV}$ and $p_T(\mu^\pm e^\mp) > 130\text{ GeV}$, are used in the limit setting procedure for the 8 TeV analysis. The bin boundaries are chosen such that the a priori expectation for SM $\gamma\gamma \rightarrow W^+W^-$ in the highest bin is ~ 0.1 events, with other backgrounds, predominantly electroweak W^+W^- production, contributing an additional ~ 0.1 events. In the 7 TeV analysis [5] a single bin with $p_T(\mu^\pm e^\mp) > 100\text{ GeV}$ was used, also chosen such that the a priori expectation for SM $\gamma\gamma \rightarrow W^+W^-$ is ~ 0.1 events.

In both the 7 and 8 TeV analyses, and in the combination, the Feldman–Cousins prescription [66] is used to derive limits. In the 7 TeV analysis, where the number of expected and observed events was near zero, the inclusion of systematic uncertainties in the background estimate resulted in a shortening of the 95% confidence interval. Therefore a conservative procedure of integrating the systematic uncertainties out, reproducing the method advocated by Cousins and Highland [67], was used. In the 8 TeV analysis and in the 7+8 TeV combination, no such effect is observed, therefore the systematic uncertainties are included as log-normal nuisance parameters in the limit calculation. As in the case of the combined significance calculations, the systematic uncertainties are treated as uncorrelated between the two data sets, except for the EPA uncertainty, which is fully correlated.

Table 3 summarizes all of the limits on the dimension-6 and dimension-8 AQGC parameters obtained from the 7 and 8 TeV $\gamma\gamma \rightarrow W^+W^-$ data separately, and from the combination of the two. The 7 TeV dimension-6 results are taken from Ref. [5], and translated into the dimension-8 formalism as described in Section 2, using Eq. (1). For these limits all parameters except the one shown are fixed to zero (the value expected in the standard model). The 8 TeV results are an improvement over previously published values with $\Lambda_{\text{cutoff}} = 500\text{ GeV}$ [5, 19, 21], of which the CMS 7 TeV limits of $1.5 \times 10^{-4}\text{ GeV}^{-2}$ and $5 \times 10^{-4}\text{ GeV}^{-2}$ on a_0^W/Λ^2 and a_C^W/Λ^2 , respectively, are the most stringent. These limits are also approximately two orders of magnitude more stringent than those obtained at LEP [12–18], where unitarity was approximately preserved without form factors, due to the lower \sqrt{s} of e^+e^- collisions. By combining the 7 and 8 TeV data sets, we find upper limits at 95% CL that are $\sim 10\%$ more restrictive than the 8 TeV results alone, for the case of a dipole form factor with $\Lambda_{\text{cutoff}} = 500\text{ GeV}$.

With no form factor corrections, there is nothing to prevent the rapidly increasing cross section from violating unitarity at high energies in the theory. We also obtain exclusion results in this scenario, listed in Table 3, for comparison with other unitarity-violating limits on the same operators [5, 19–21, 23]. In this case the high-energy behavior leads to a larger improvement when comparing the 8 TeV to the 7 TeV results in the $\gamma\gamma \rightarrow W^+W^-$ channel. The dominance of the 8 TeV results in the unitarity-violating limits also results in only a very small improvement when they are combined with the 7 TeV limits.

We perform a similar procedure to derive two-dimensional limits in the $(a_0^W/\Lambda^2, a_C^W/\Lambda^2)$ parameter space for the unitarized results with $\Lambda_{\text{cutoff}} = 500\text{ GeV}$. The two-dimensional 95% confidence level exclusion regions obtained from $\gamma\gamma \rightarrow W^+W^-$ production at CMS are shown in Fig. 10 for the 7 TeV data (from Ref. [5]), the 8 TeV data, and from the final 7 and 8 TeV combination.

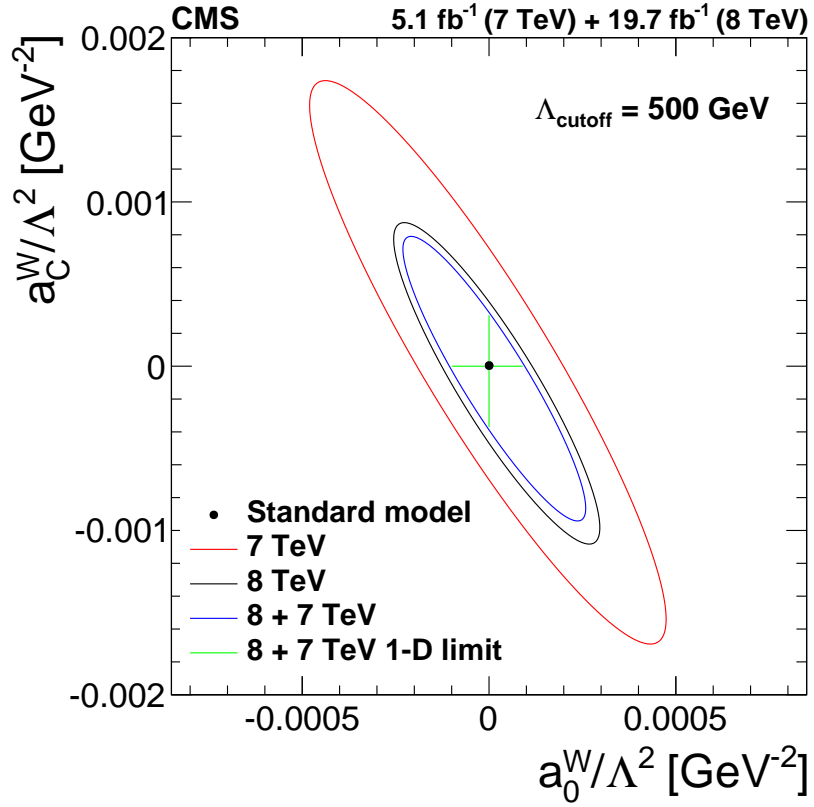


Figure 10: Excluded values of the anomalous coupling parameters a_0^W/Λ^2 and a_C^W/Λ^2 with $\Lambda_{\text{cutoff}} = 500 \text{ GeV}$. The exclusion regions are shown for the CMS measurements of $\gamma\gamma \rightarrow W^+W^-$ at 7 TeV (outer contour), 8 TeV (middle contour), and the 7+8 TeV combination (innermost contour). The areas outside the solid contours are excluded by each measurement at 95% CL. The cross indicates the one-dimensional limits obtained for each parameter from the 7 and 8 TeV combination, with the other parameter fixed to zero.

Table 3: Summary of all 95% CL AQGC limits derived from the measured $p_T(\mu e)$ distributions in the $\gamma\gamma \rightarrow W^+W^-$ signal region production in CMS at 7 and 8 TeV. The second column lists the 7 TeV limits on dimension-6 operators taken from Ref. [5], as well as their conversion to dimension-8 operators at 7 TeV. The third column contains the 8 TeV results described in this paper. The final column shows the combined 7 and 8 TeV limits.

Dimension-6 AQGC parameter	7 TeV ($\times 10^{-4} \text{ GeV}^{-2}$)	8 TeV ($\times 10^{-4} \text{ GeV}^{-2}$)	7+8 TeV ($\times 10^{-4} \text{ GeV}^{-2}$)
$a_0^W/\Lambda^2(\Lambda_{\text{cutoff}} = 500 \text{ GeV})$	$-1.5 < a_0^W/\Lambda^2 < 1.5$	$-1.1 < a_0^W/\Lambda^2 < 1.0$	$-0.9 < a_0^W/\Lambda^2 < 0.9$
$a_C^W/\Lambda^2(\Lambda_{\text{cutoff}} = 500 \text{ GeV})$	$-5 < a_C^W/\Lambda^2 < 5$	$-4.2 < a_C^W/\Lambda^2 < 3.4$	$-3.6 < a_C^W/\Lambda^2 < 3.0$
Dimension-8 AQGC parameter	7 TeV ($\times 10^{-10} \text{ GeV}^{-4}$)	8 TeV ($\times 10^{-10} \text{ GeV}^{-4}$)	7+8 TeV ($\times 10^{-10} \text{ GeV}^{-4}$)
$f_{M,0}/\Lambda^4(\Lambda_{\text{cutoff}} = 500 \text{ GeV})$	$-5.7 < f_{M,0}/\Lambda^4 < 5.7$	$-3.8 < f_{M,0}/\Lambda^4 < 4.2$	$-3.4 < f_{M,0}/\Lambda^4 < 3.4$
$f_{M,1}/\Lambda^4(\Lambda_{\text{cutoff}} = 500 \text{ GeV})$	$-19 < f_{M,1}/\Lambda^4 < 19$	$-16 < f_{M,1}/\Lambda^4 < 13$	$-14 < f_{M,1}/\Lambda^4 < 12$
$f_{M,2}/\Lambda^4(\Lambda_{\text{cutoff}} = 500 \text{ GeV})$	$-2.8 < f_{M,2}/\Lambda^4 < 2.8$	$-1.9 < f_{M,2}/\Lambda^4 < 2.1$	$-1.9 < f_{M,2}/\Lambda^4 < 1.9$
$f_{M,3}/\Lambda^4(\Lambda_{\text{cutoff}} = 500 \text{ GeV})$	$-9.5 < f_{M,3}/\Lambda^4 < 9.5$	$-8.0 < f_{M,3}/\Lambda^4 < 6.5$	$-6.8 < f_{M,3}/\Lambda^4 < 5.7$
Dimension-6 AQGC parameter	7 TeV ($\times 10^{-6} \text{ GeV}^{-2}$)	8 TeV ($\times 10^{-6} \text{ GeV}^{-2}$)	7+8 TeV ($\times 10^{-6} \text{ GeV}^{-2}$)
$a_0^W/\Lambda^2(\text{no form factor})$	$-4 < a_0^W/\Lambda^2 < 4$	$-1.2 < a_0^W/\Lambda^2 < 1.2$	$-1.1 < a_0^W/\Lambda^2 < 1.1$
$a_C^W/\Lambda^2(\text{no form factor})$	$-15 < a_C^W/\Lambda^2 < 15$	$-4.4 < a_C^W/\Lambda^2 < 4.4$	$-4.1 < a_C^W/\Lambda^2 < 4.1$
Dimension-8 AQGC parameter	7 TeV ($\times 10^{-12} \text{ GeV}^{-4}$)	8 TeV ($\times 10^{-12} \text{ GeV}^{-4}$)	7+8 TeV ($\times 10^{-12} \text{ GeV}^{-4}$)
$f_{M,0}/\Lambda^4(\text{no form factor})$	$-15 < f_{M,0}/\Lambda^4 < 15$	$-4.6 < f_{M,0}/\Lambda^4 < 4.6$	$-4.2 < f_{M,0}/\Lambda^4 < 4.2$
$f_{M,1}/\Lambda^4(\text{no form factor})$	$-57 < f_{M,1}/\Lambda^4 < 57$	$-17 < f_{M,1}/\Lambda^4 < 17$	$-16 < f_{M,1}/\Lambda^4 < 16$
$f_{M,2}/\Lambda^4(\text{no form factor})$	$-7.6 < f_{M,2}/\Lambda^4 < 7.6$	$-2.3 < f_{M,2}/\Lambda^4 < 2.3$	$-2.1 < f_{M,2}/\Lambda^4 < 2.1$
$f_{M,3}/\Lambda^4(\text{no form factor})$	$-28 < f_{M,3}/\Lambda^4 < 28$	$-8.4 < f_{M,3}/\Lambda^4 < 8.4$	$-7.8 < f_{M,3}/\Lambda^4 < 7.8$

10 Conclusions

Results are presented for exclusive and quasi-exclusive $\gamma\gamma \rightarrow W^+W^-$ production in the $\mu^\pm e^\mp$ final state in pp collisions at $\sqrt{s} = 8$ (7) TeV, using data samples corresponding to integrated luminosities of 19.7 (5.05) fb^{-1} . In the signal region with $p_T(\mu^\pm e^\mp) > 30$ GeV and no additional charged particles associated with the $\mu^\pm e^\mp$ vertex, we observe 13 (2) events with an expected background of 3.9 ± 0.6 (0.84 ± 0.15) events in the 8 (7) TeV data. The observed yields and kinematic distributions are consistent with the SM prediction, with a combined significance over the background-only hypothesis of 3.4σ . No significant deviations from the SM are observed in the $p_T(\mu^\pm e^\mp)$ distribution, and the combined 7+8 TeV limits are interpreted in terms of improved constraints on dimension-6 and dimension-8 anomalous quartic gauge operator couplings.

Acknowledgments

We congratulate our colleagues in the CERN accelerator departments for the excellent performance of the LHC and thank the technical and administrative staffs at CERN and at other CMS institutes for their contributions to the success of the CMS effort. In addition, we gratefully acknowledge the computing centers and personnel of the Worldwide LHC Computing Grid for delivering so effectively the computing infrastructure essential to our analyses. Finally, we acknowledge the enduring support for the construction and operation of the LHC and the CMS detector provided by the following funding agencies: the Austrian Federal Ministry of Science, Research and Economy and the Austrian Science Fund; the Belgian Fonds de la Recherche Scientifique, and Fonds voor Wetenschappelijk Onderzoek; the Brazilian Funding Agencies (CNPq, CAPES, FAPERJ, and FAPESP); the Bulgarian Ministry of Education and Science; CERN; the Chinese Academy of Sciences, Ministry of Science and Technology, and National Natural Science Foundation of China; the Colombian Funding Agency (COLCIENCIAS);

the Croatian Ministry of Science, Education and Sport, and the Croatian Science Foundation; the Research Promotion Foundation, Cyprus; the Ministry of Education and Research, Estonian Research Council via IUT23-4 and IUT23-6 and European Regional Development Fund, Estonia; the Academy of Finland, Finnish Ministry of Education and Culture, and Helsinki Institute of Physics; the Institut National de Physique Nucléaire et de Physique des Particules / CNRS, and Commissariat à l'Énergie Atomique et aux Énergies Alternatives / CEA, France; the Bundesministerium für Bildung und Forschung, Deutsche Forschungsgemeinschaft, and Helmholtz-Gemeinschaft Deutscher Forschungszentren, Germany; the General Secretariat for Research and Technology, Greece; the National Scientific Research Foundation, and National Innovation Office, Hungary; the Department of Atomic Energy and the Department of Science and Technology, India; the Institute for Studies in Theoretical Physics and Mathematics, Iran; the Science Foundation, Ireland; the Istituto Nazionale di Fisica Nucleare, Italy; the Ministry of Science, ICT and Future Planning, and National Research Foundation (NRF), Republic of Korea; the Lithuanian Academy of Sciences; the Ministry of Education, and University of Malaya (Malaysia); the Mexican Funding Agencies (CINVESTAV, CONACYT, SEP, and UASLP-FAI); the Ministry of Business, Innovation and Employment, New Zealand; the Pakistan Atomic Energy Commission; the Ministry of Science and Higher Education and the National Science Centre, Poland; the Fundação para a Ciência e a Tecnologia, Portugal; JINR, Dubna; the Ministry of Education and Science of the Russian Federation, the Federal Agency of Atomic Energy of the Russian Federation, Russian Academy of Sciences, and the Russian Foundation for Basic Research; the Ministry of Education, Science and Technological Development of Serbia; the Secretaría de Estado de Investigación, Desarrollo e Innovación and Programa Consolider-Ingenio 2010, Spain; the Swiss Funding Agencies (ETH Board, ETH Zurich, PSI, SNF, UniZH, Canton Zurich, and SER); the Ministry of Science and Technology, Taipei; the Thailand Center of Excellence in Physics, the Institute for the Promotion of Teaching Science and Technology of Thailand, Special Task Force for Activating Research and the National Science and Technology Development Agency of Thailand; the Scientific and Technical Research Council of Turkey, and Turkish Atomic Energy Authority; the National Academy of Sciences of Ukraine, and State Fund for Fundamental Researches, Ukraine; the Science and Technology Facilities Council, UK; the US Department of Energy, and the US National Science Foundation.

Individuals have received support from the Marie-Curie program and the European Research Council and EPLANET (European Union); the Leventis Foundation; the A. P. Sloan Foundation; the Alexander von Humboldt Foundation; the Belgian Federal Science Policy Office; the Fonds pour la Formation à la Recherche dans l'Industrie et dans l'Agriculture (FRRIA-Belgium); the Agentschap voor Innovatie door Wetenschap en Technologie (IWT-Belgium); the Ministry of Education, Youth and Sports (MEYS) of the Czech Republic; the Council of Science and Industrial Research, India; the HOMING PLUS program of the Foundation for Polish Science, cofinanced from European Union, Regional Development Fund; the Mobility Plus program of the Ministry of Science and Higher Education (Poland); the OPUS program of the National Science Center (Poland); MIUR project 20108T4XTM (Italy); the Thalís and Aristeia programs cofinanced by EU-ESF and the Greek NSRF; the National Priorities Research Program by Qatar National Research Fund; the Rachadapisek Sompot Fund for Postdoctoral Fellowship, Chulalongkorn University (Thailand); the Chulalongkorn Academic into Its 2nd Century Project Advancement Project (Thailand); and the Welch Foundation, contract C-1845.

References

- [1] J. de Favereau de Jeneret et al., "High energy photon interactions at the LHC", (2009).
arXiv:0908.2020.

- [2] CMS Collaboration, “Exclusive photon-photon production of muon pairs in proton-proton collisions at $\sqrt{s} = 7$ TeV”, *JHEP* **01** (2012) 052, doi:10.1007/JHEP01(2012)052, arXiv:1111.5536.
- [3] ATLAS Collaboration, “Measurement of exclusive $\gamma\gamma \rightarrow \ell^+\ell^-$ production in proton-proton collisions at $\sqrt{s} = 7$ TeV with the ATLAS detector”, *Phys. Lett. B* **749** (2015) 242, doi:10.1016/j.physletb.2015.07.069, arXiv:1506.07098.
- [4] CMS Collaboration, “Search for exclusive or semi-exclusive photon pair production and observation of exclusive and semi-exclusive electron pair production in pp collisions at $\sqrt{s} = 7$ TeV”, *JHEP* **11** (2012) 080, doi:10.1007/JHEP11(2012)080, arXiv:1209.1666.
- [5] CMS Collaboration, “Study of exclusive two-photon production of W^+W^- in pp collisions at $\sqrt{s} = 7$ TeV and constraints on anomalous quartic gauge couplings”, *JHEP* **07** (2013) 116, doi:10.1007/JHEP07(2013)116, arXiv:1305.5596.
- [6] T. Pierzchala and K. Piotrkowski, “Sensitivity to anomalous quartic gauge couplings in photon-photon interactions at the LHC”, *Nucl. Phys. Proc. Suppl.* **179** (2008) 257, doi:10.1016/j.nuclphysbps.2008.07.032, arXiv:0807.1121.
- [7] E. Chapon, C. Royon, and O. Kepka, “Anomalous quartic $WW\gamma\gamma$, $ZZ\gamma\gamma$, and trilinear $WW\gamma$ couplings in two-photon processes at high luminosity at the LHC”, *Phys. Rev. D* **81** (2010) 074003, doi:10.1103/PhysRevD.81.074003, arXiv:0912.5161.
- [8] M. Maniatis, A. von Manteuffel, and O. Nachtmann, “Anomalous couplings in $\gamma\gamma \rightarrow W^+W^-$ at LHC and ILC”, *Nucl. Phys. Proc. Suppl.* **179** (2008) 104, doi:10.1016/j.nuclphysbps.2008.07.012.
- [9] R. L. Delgado, A. Dobado, M. J. Herrero, and J. J. Sanz-Cillero, “One-loop $\gamma\gamma \rightarrow W_L^+W_L^-$ and $\gamma\gamma \rightarrow Z_L Z_L$ from the electroweak chiral lagrangian with a light Higgs-like scalar”, *JHEP* **07** (2014) 149, doi:10.1007/JHEP07(2014)149, arXiv:1404.2866.
- [10] S. Fichet and G. von Gersdorff, “Anomalous gauge couplings from composite Higgs and warped extra dimensions”, *JHEP* **03** (2014) 102, doi:10.1007/JHEP03(2014)102, arXiv:1311.6815.
- [11] D. Espriu and F. Mescia, “Unitarity and causality constraints in composite Higgs models”, *Phys. Rev. D* **90** (2014) 015035, doi:10.1103/PhysRevD.90.015035, arXiv:1403.7386.
- [12] ALEPH Collaboration, “Constraints on anomalous QGC’s in e^+e^- interactions from 183 GeV to 209 GeV”, *Phys. Lett. B* **602** (2004) 31, doi:10.1016/j.physletb.2004.09.041.
- [13] OPAL Collaboration, “Constraints on anomalous quartic gauge boson couplings from $\nu\bar{\nu}\gamma\gamma$ and $q\bar{q}\gamma\gamma$ events at LEP-2”, *Phys. Rev. D* **70** (2004) 032005, doi:10.1103/PhysRevD.70.032005, arXiv:hep-ex/0402021.
- [14] OPAL Collaboration, “A study of $W^+W^-\gamma$ events at LEP”, *Phys. Lett. B* **580** (2004) 17, doi:10.1016/j.physletb.2003.10.063, arXiv:hep-ex/0309013.
- [15] OPAL Collaboration, “Measurement of the $W^+W^-\gamma$ cross-section and first direct limits on anomalous electroweak quartic gauge couplings”, *Phys. Lett. B* **471** (1999) 293, doi:10.1016/S0370-2693(99)01357-X, arXiv:hep-ex/9910069.

- [16] DELPHI Collaboration, "Measurement of the $e^+e^- \rightarrow W^+W^-\gamma$ cross-section and limits on anomalous quartic gauge couplings with DELPHI", *Eur. Phys. J. C* **31** (2003) 139, doi:10.1140/epjc/s2003-01350-x, arXiv:hep-ex/0311004.
- [17] L3 Collaboration, "The $e^+e^- \rightarrow Z\gamma\gamma \rightarrow q\bar{q}\gamma\gamma$ reaction at LEP and constraints on anomalous quartic gauge boson couplings", *Phys. Lett. B* **540** (2002) 43, doi:10.1016/S0370-2693(02)02127-5, arXiv:hep-ex/0206050.
- [18] L3 Collaboration, "Study of the $W^+W^-\gamma$ process and limits on anomalous quartic gauge boson couplings at LEP", *Phys. Lett. B* **527** (2002) 29, doi:10.1016/S0370-2693(02)01167-X, arXiv:hep-ex/0111029.
- [19] D0 Collaboration, "Search for anomalous quartic $WW\gamma\gamma$ couplings in dielectron and missing energy final states in $p\bar{p}$ collisions at $\sqrt{s} = 1.96$ TeV", *Phys. Rev. D* **88** (2013) 012005, doi:10.1103/PhysRevD.88.012005, arXiv:1305.1258.
- [20] CMS Collaboration, "A search for WW gamma and WZ gamma production and constraints on anomalous quartic gauge couplings in pp collisions at $\sqrt{s} = 8$ TeV", *Phys. Rev. D* **90** (2014) 032008, doi:10.1103/PhysRevD.90.032008, arXiv:1404.4619.
- [21] ATLAS Collaboration, "Evidence of $W\gamma\gamma$ production in pp collisions at $\sqrt{s} = 8$ TeV and limits on anomalous quartic gauge couplings with the ATLAS Detector", *Phys. Rev. Lett.* **115** (2015) 031802, doi:10.1103/PhysRevLett.115.031802, arXiv:1503.03243.
- [22] ATLAS Collaboration, "Evidence for electroweak production of $W^\pm W^\pm jj$ in pp collisions at $\sqrt{s} = 8$ TeV with the ATLAS detector", *Phys. Rev. Lett.* **113** (2014) 141803, doi:10.1103/PhysRevLett.113.141803, arXiv:1405.6241.
- [23] CMS Collaboration, "Study of vector boson scattering and search for new physics in events with two same-sign leptons and two jets", *Phys. Rev. Lett.* **114** (2015) 051801, doi:10.1103/PhysRevLett.114.051801, arXiv:1410.6315.
- [24] V. A. Khoze, A. D. Martin, R. Orava, and M. G. Ryskin, "Luminosity monitors at the LHC", *Eur. Phys. J. C* **19** (2001) 313, doi:10.1007/s100520100616, arXiv:hep-ph/0010163.
- [25] L. A. Harland-Lang, V. A. Khoze, M. G. Ryskin, and W. J. Stirling, "The phenomenology of central exclusive production at hadron colliders", *Eur. Phys. J. C* **72** (2012) 2110, doi:10.1140/epjc/s10052-012-2110-2, arXiv:1204.4803.
- [26] G. Belanger and F. Boudjema, "Probing quartic couplings of weak bosons through three vectors production at a 500 GeV NLC", *Phys. Lett. B* **288** (1992) 201, doi:10.1016/0370-2693(92)91978-I.
- [27] ATLAS Collaboration, "Observation of a new particle in the search for the Standard Model Higgs boson with the ATLAS detector at the LHC", *Phys. Lett. B* **716** (2012) 1, doi:10.1016/j.physletb.2012.08.020, arXiv:1207.7214.
- [28] CMS Collaboration, "Observation of a new boson at a mass of 125 GeV with the CMS experiment at the LHC", *Phys. Lett. B* **716** (2012) 30, doi:10.1016/j.physletb.2012.08.021, arXiv:1207.7235.

- [29] CMS Collaboration, “Observation of a new boson with mass near 125 GeV in pp collisions at $\sqrt{s} = 7$ and 8 TeV”, *JHEP* **06** (2013) 081, doi:10.1007/JHEP06(2013)081, arXiv:1303.4571.
- [30] G. Belanger et al., “Bosonic quartic couplings at LEP-2”, *Eur. Phys. J. C* **13** (2000) 283, doi:10.1007/s100520000305, arXiv:hep-ph/9908254.
- [31] O. J. P. Eboli, M. C. Gonzalez-Garcia, and J. K. Mizukoshi, “ $pp \rightarrow jje^\pm\mu^\pm\nu\nu$ and $jje^\pm\mu^\mp\nu\nu$ at $O(\alpha_{em}^6)$ and $O(\alpha_{em}^4\alpha_s^2)$ for the study of the quartic electroweak gauge boson vertex at CERN LHC”, *Phys. Rev. D* **74** (2006) 073005, doi:10.1103/PhysRevD.74.073005, arXiv:hep-ph/0606118.
- [32] M. Baak et al., “Working group report: precision study of electroweak interactions”, (2013). arXiv:1310.6708.
- [33] O. J. P. Eboli, M. C. Gonzalez-Garcia, S. M. Lietti, and S. F. Novaes, “Anomalous quartic gauge boson couplings at hadron colliders”, *Phys. Rev. D* **63** (2001) 075008, doi:10.1103/PhysRevD.63.075008, arXiv:hep-ph/0009262.
- [34] R. S. Gupta, “Probing quartic neutral gauge boson couplings using diffractive photon fusion at the LHC”, *Phys. Rev. D* **85** (2012) 014006, doi:10.1103/PhysRevD.85.014006, arXiv:1111.3354.
- [35] A. Alboteanu, W. Kilian, and J. Reuter, “Resonances and unitarity in weak boson scattering at the LHC”, *JHEP* **11** (2008) 010, doi:10.1088/1126-6708/2008/11/010, arXiv:0806.4145.
- [36] CMS Collaboration, “The CMS experiment at the CERN LHC”, *JINST* **3** (2008) S08004, doi:10.1088/1748-0221/3/08/S08004.
- [37] CMS Collaboration, “Performance of electron reconstruction and selection with the CMS detector in proton-proton collisions at $\sqrt{s} = 8$ TeV”, *JINST* **10** (2015) P06005, doi:10.1088/1748-0221/10/06/P06005, arXiv:1502.02701.
- [38] CMS Collaboration, “Description and performance of track and primary-vertex reconstruction with the CMS tracker”, *JINST* **9** (2014) P10009, doi:10.1088/1748-0221/9/10/P10009, arXiv:1405.6569.
- [39] J. Alwall et al., “MadGraph 5: going beyond”, *JHEP* **06** (2011) 128, doi:10.1007/JHEP06(2011)128, arXiv:1106.0522.
- [40] J. Alwall et al., “The automated computation of tree-level and next-to-leading order differential cross sections, and their matching to parton shower simulations”, *JHEP* **07** (2014) 079, doi:10.1007/JHEP07(2014)079, arXiv:1405.0301.
- [41] V. M. Budnev, I. F. Ginzburg, G. V. Meledin, and V. G. Serbo, “The two-photon particle production mechanism. Physical problems. Applications. Equivalent photon approximation”, *Phys. Rept.* **15** (1975) 181, doi:10.1016/0370-1573(75)90009-5.
- [42] A. Belyaev, N. D. Christensen, and A. Pukhov, “CalcHEP 3.4 for collider physics within and beyond the Standard Model”, *Comput. Phys. Commun.* **184** (2013) 1729, doi:10.1016/j.cpc.2013.01.014, arXiv:1207.6082.
- [43] J. A. M. Vermaseren, “Two-photon processes at very high energies”, *Nucl. Phys. B* **229** (1983) 347, doi:10.1016/0550-3213(83)90336-X.

- [44] S. P. Baranov, O. Duenger, H. Shooshtari, and J. A. M. Vermaseren, "LPAIR: A generator for lepton pair production", in *Proceedings of Physics at HERA*, volume 3, p. 1478. 1991.
- [45] M. Czakon and A. Mitov, "Top++: a program for the calculation of the top-pair cross-section at hadron colliders", *Comput. Phys. Commun.* **185** (2014) 2930, doi:10.1016/j.cpc.2014.06.021, arXiv:1112.5675.
- [46] J. M. Campbell and R. K. Ellis, "MCFM for the Tevatron and the LHC", *Nucl. Phys. Proc. Suppl.* **205** (2010) 10, doi:10.1016/j.nuclphysbps.2010.08.011, arXiv:1007.3492.
- [47] P. Nason, "A new method for combining NLO QCD with shower Monte Carlo algorithms", *JHEP* **11** (2004) 040, doi:10.1088/1126-6708/2004/11/040, arXiv:hep-ph/0409146.
- [48] S. Frixione, P. Nason, and C. Oleari, "Matching NLO QCD computations with parton shower simulations: the POWHEG method", *JHEP* **11** (2007) 070, doi:10.1088/1126-6708/2007/11/070, arXiv:0709.2092.
- [49] S. Alioli, P. Nason, C. Oleari, and E. Re, "A general framework for implementing NLO calculations in shower Monte Carlo programs: the POWHEG BOX", *JHEP* **06** (2010) 043, doi:10.1007/JHEP06(2010)043, arXiv:1002.2581.
- [50] T. Sjöstrand, S. Mrenna, and P. Z. Skands, "PYTHIA 6.4 Physics and Manual", *JHEP* **05** (2006) 026, doi:10.1088/1126-6708/2006/05/026, arXiv:hep-ph/0603175.
- [51] CMS Collaboration, "Study of the underlying event at forward rapidity in pp collisions at $\sqrt{s} = 0.9, 2.76, \text{ and } 7 \text{ TeV}$ ", *JHEP* **04** (2013) 072, doi:10.1007/JHEP04(2013)072, arXiv:1302.2394.
- [52] R. Field, "Min-bias and the underlying event at the LHC", *Acta Phys. Polon. B* **42** (2011) 2631, doi:10.5506/APhysPolB.42.2631, arXiv:1110.5530.
- [53] P. Bruni and G. Ingelman, "Diffractive hard scattering at ep and p \bar{p} colliders", in *Proceedings of the Int. Europhysics Conf. on High Energy Physics*, J. Carr and M. Perrottet, eds., p. 595. Ed. Frontières, Marseille, France, 1994.
- [54] H1 Collaboration, "Measurement and QCD analysis of the diffractive deep-inelastic scattering cross-section at HERA", *Eur. Phys. J. C* **48** (2006) 715, doi:10.1140/epjc/s10052-006-0035-3, arXiv:hep-ex/0606004.
- [55] CMS Collaboration, "Observation of a diffractive contribution to dijet production in proton-proton collisions at $\sqrt{s} = 7 \text{ TeV}$ ", *Phys. Rev. D* **87** (2013) 012006, doi:10.1103/PhysRevD.87.012006, arXiv:1209.1805.
- [56] P. Lebiedowicz, R. Pasechnik, and A. Szczurek, "QCD diffractive mechanism of exclusive W^+W^- pair production at high energies", *Nucl. Phys. B* **867** (2013) 61, doi:10.1016/j.nuclphysb.2012.09.014, arXiv:1203.1832.
- [57] CMS Collaboration, "Measurement of electroweak production of two jets in association with a Z boson in proton-proton collisions at $\sqrt{s} = 8 \text{ TeV}$ ", *Eur. Phys. J. C* **75** (2015) 66, doi:10.1140/epjc/s10052-014-3232-5, arXiv:1410.3153.

- [58] A. Ballestrero et al., “PHANTOM: A Monte Carlo event generator for six parton final states at high energy colliders”, *Comput. Phys. Commun.* **180** (2009) 401, doi:10.1016/j.cpc.2008.10.005, arXiv:0801.3359.
- [59] GEANT4 Collaboration, “GEANT4—a simulation toolkit”, *Nucl. Instrum. Meth. A* **506** (2003) 250, doi:10.1016/S0168-9002(03)01368-8.
- [60] CMS Collaboration, “Performance of CMS muon reconstruction in pp collision events at $\sqrt{s} = 7$ TeV”, *JINST* **7** (2012) P10002, doi:10.1088/1748-0221/7/10/P10002, arXiv:1206.4071.
- [61] CMS Collaboration, “Particle-Flow Event Reconstruction in CMS and Performance for Jets, Taus, and E_T^{miss} ”, CMS Physics Analysis Summary CMS-PAS-PFT-09-001, 2009.
- [62] CMS Collaboration, “Commissioning of the Particle-flow Event Reconstruction with the first LHC collisions recorded in the CMS detector”, CMS Physics Analysis Summary CMS-PAS-PFT-10-001, 2010.
- [63] G. G. da Silveira et al., “Central $\mu^+ \mu^-$ production via photon-photon fusion in proton-proton collisions with proton dissociation”, *JHEP* **02** (2015) 159, doi:10.1007/JHEP02(2015)159, arXiv:1409.1541.
- [64] L. A. Harland-Lang, V. A. Khoze, and M. G. Ryskin, “The photon PDF in events with rapidity gaps”, *Eur. Phys. J.* **C76** (2016), no. 5, 255, doi:10.1140/epjc/s10052-016-4100-2, arXiv:1601.03772.
- [65] CMS Collaboration, “CMS Luminosity Based on Pixel Cluster Counting - Summer 2013 Update”, CMS Physics Analysis Summary CMS-PAS-LUM-13-001, 2013.
- [66] G. J. Feldman and R. D. Cousins, “A unified approach to the classical statistical analysis of small signals”, *Phys. Rev. D* **57** (1998) 3873, doi:10.1103/PhysRevD.57.3873, arXiv:physics/9711021.
- [67] R. D. Cousins and V. L. Highland, “Incorporating systematic uncertainties into an upper limit”, *Nucl. Instrum. Meth. A* **320** (1992) 331, doi:10.1016/0168-9002(92)90794-5.

A The CMS Collaboration

Yerevan Physics Institute, Yerevan, Armenia

V. Khachatryan, A.M. Sirunyan, A. Tumasyan

Institut für Hochenergiephysik der OeAW, Wien, Austria

W. Adam, E. Asilar, T. Bergauer, J. Brandstetter, E. Brondolin, M. Dragicevic, J. Erö, M. Flechl, M. Friedl, R. Frühwirth¹, V.M. Ghete, C. Hartl, N. Hörmann, J. Hrubec, M. Jeitler¹, V. Knünz, A. König, M. Krammer¹, I. Krätschmer, D. Liko, T. Matsushita, I. Mikulec, D. Rabadý², N. Rad, B. Rahbaran, H. Rohringer, J. Schieck¹, R. Schöfbeck, J. Strauss, W. Treberer-Treberspurg, W. Waltenberger, C.-E. Wulz¹

National Centre for Particle and High Energy Physics, Minsk, Belarus

V. Mossolov, N. Shumeiko, J. Suarez Gonzalez

Universiteit Antwerpen, Antwerpen, Belgium

S. Alderweireldt, T. Cornelis, E.A. De Wolf, X. Janssen, A. Knutsson, J. Lauwers, S. Luyckx, M. Van De Klundert, H. Van Haevermaet, P. Van Mechelen, N. Van Remortel, A. Van Spilbeeck

Vrije Universiteit Brussel, Brussel, Belgium

S. Abu Zeid, F. Blekman, J. D'Hondt, N. Daci, I. De Bruyn, K. Deroover, N. Heracleous, J. Keaveney, S. Lowette, L. Moreels, A. Olbrechts, Q. Python, D. Strom, S. Tavernier, W. Van Doninck, P. Van Mulders, G.P. Van Onsem, I. Van Parijs

Université Libre de Bruxelles, Bruxelles, Belgium

P. Barria, H. Brun, C. Caillol, B. Clerboux, G. De Lentdecker, W. Fang, G. Fasanella, L. Favart, R. Goldouzian, A. Grebenyuk, G. Karapostoli, T. Lenzi, A. Léonard, T. Maerschalk, A. Marinov, L. Perniè, A. Randle-conde, T. Seva, C. Vander Velde, P. Vanlaer, R. Yonamine, F. Zenoni, F. Zhang³

Ghent University, Ghent, Belgium

K. Beernaert, L. Benucci, A. Cimmino, S. Crucy, D. Dobur, A. Fagot, G. Garcia, M. Gul, J. Mccartin, A.A. Ocampo Rios, D. Poyraz, D. Ryckbosch, S. Salva, M. Sigamani, M. Tytgat, W. Van Driessche, E. Yazgan, N. Zaganidis

Université Catholique de Louvain, Louvain-la-Neuve, Belgium

S. Basegmez, C. Beluffi⁴, O. Bondu, S. Brochet, G. Bruno, A. Caudron, L. Ceard, S. De Visscher, C. Delaere, M. Delcourt, D. Favart, L. Forthomme, A. Giammanco, A. Jafari, P. Jez, M. Komm, V. Lemaître, A. Mertens, M. Musich, C. Nuttens, L. Perrini, K. Piotrkowski, A. Popov⁵, L. Quertenmont, M. Selvaggi, M. Vidal Marono

Université de Mons, Mons, Belgium

N. Belyi, G.H. Hammad

Centro Brasileiro de Pesquisas Físicas, Rio de Janeiro, Brazil

W.L. Aldá Júnior, F.L. Alves, G.A. Alves, L. Brito, M. Correa Martins Junior, M. Hamer, C. Hensel, A. Moraes, M.E. Pol, P. Rebello Teles

Universidade do Estado do Rio de Janeiro, Rio de Janeiro, Brazil

E. Belchior Batista Das Chagas, W. Carvalho, J. Chinellato⁶, A. Custódio, E.M. Da Costa, D. De Jesus Damiao, C. De Oliveira Martins, S. Fonseca De Souza, L.M. Huertas Guativa, H. Malbouisson, D. Matos Figueiredo, C. Mora Herrera, L. Mundim, H. Nogima, W.L. Prado Da Silva, A. Santoro, A. Sznajder, E.J. Tonelli Manganote⁶, A. Vilela Pereira

Universidade Estadual Paulista ^a, Universidade Federal do ABC ^b, São Paulo, Brazil

S. Ahuja^a, C.A. Bernardes^b, A. De Souza Santos^b, S. Dogra^a, T.R. Fernandez Perez Tomei^a, E.M. Gregores^b, P.G. Mercadante^b, C.S. Moon^{a,7}, S.F. Novaes^a, Sandra S. Padula^a, D. Romero Abad^b, J.C. Ruiz Vargas

Institute for Nuclear Research and Nuclear Energy, Sofia, Bulgaria

A. Aleksandrov, R. Hadjiiska, P. Iaydjiev, M. Rodozov, S. Stoykova, G. Sultanov, M. Vutova

University of Sofia, Sofia, Bulgaria

A. Dimitrov, I. Glushkov, L. Litov, B. Pavlov, P. Petkov

Institute of High Energy Physics, Beijing, China

M. Ahmad, J.G. Bian, G.M. Chen, H.S. Chen, M. Chen, T. Cheng, R. Du, C.H. Jiang, D. Leggat, R. Plestina⁸, F. Romeo, S.M. Shaheen, A. Spiezia, J. Tao, C. Wang, Z. Wang, H. Zhang

State Key Laboratory of Nuclear Physics and Technology, Peking University, Beijing, China

C. Asawatangtrakuldee, Y. Ban, Q. Li, S. Liu, Y. Mao, S.J. Qian, D. Wang, Z. Xu

Universidad de Los Andes, Bogota, Colombia

C. Avila, A. Cabrera, L.F. Chaparro Sierra, C. Florez, J.P. Gomez, B. Gomez Moreno, J.C. Sanabria

University of Split, Faculty of Electrical Engineering, Mechanical Engineering and Naval Architecture, Split, Croatia

N. Godinovic, D. Lelas, I. Puljak, P.M. Ribeiro Cipriano

University of Split, Faculty of Science, Split, Croatia

Z. Antunovic, M. Kovac

Institute Rudjer Boskovic, Zagreb, Croatia

V. Brigljevic, K. Kadija, J. Luetic, S. Micanovic, L. Sudic

University of Cyprus, Nicosia, Cyprus

A. Attikis, G. Mavromanolakis, J. Mousa, C. Nicolaou, F. Ptochos, P.A. Razis, H. Rykaczewski

Charles University, Prague, Czech Republic

M. Finger⁹, M. Finger Jr.⁹

Academy of Scientific Research and Technology of the Arab Republic of Egypt, Egyptian Network of High Energy Physics, Cairo, Egypt

Y. Assran^{10,11}, A. Ellithi Kamel^{12,12}, A. Mahrous¹³, A. Mohamed¹⁴

National Institute of Chemical Physics and Biophysics, Tallinn, Estonia

B. Calpas, M. Kadastik, M. Murumaa, M. Raidal, A. Tiko, C. Veelken

Department of Physics, University of Helsinki, Helsinki, Finland

P. Eerola, J. Pekkanen, M. Voutilainen

Helsinki Institute of Physics, Helsinki, Finland

J. Härkönen, V. Karimäki, R. Kinnunen, T. Lampén, K. Lassila-Perini, S. Lehti, T. Lindén, P. Luukka, T. Peltola, J. Tuominiemi, E. Tuovinen, L. Wendland

Lappeenranta University of Technology, Lappeenranta, Finland

J. Talvitie, T. Tuuva

DSM/IRFU, CEA/Saclay, Gif-sur-Yvette, France

M. Besancon, F. Couderc, M. Dejardin, D. Denegri, B. Fabbro, J.L. Faure, C. Favaro, F. Ferri,

S. Ganjour, A. Givernaud, P. Gras, G. Hamel de Monchenault, P. Jarry, E. Locci, M. Machet, J. Malcles, J. Rander, A. Rosowsky, M. Titov, A. Zghiche

Laboratoire Leprince-Ringuet, Ecole Polytechnique, IN2P3-CNRS, Palaiseau, France

A. Abdulsalam, I. Antropov, S. Baffioni, F. Beaudette, P. Busson, L. Cadamuro, E. Chapon, C. Charlot, O. Davignon, N. Filipovic, R. Granier de Cassagnac, M. Jo, S. Lisniak, L. Mastrolorenzo, P. Miné, I.N. Naranjo, M. Nguyen, C. Ochando, G. Ortona, P. Paganini, P. Pigard, S. Regnard, R. Salerno, J.B. Sauvan, Y. Sirois, T. Strebler, Y. Yilmaz, A. Zabi

Institut Pluridisciplinaire Hubert Curien, Université de Strasbourg, Université de Haute Alsace Mulhouse, CNRS/IN2P3, Strasbourg, France

J.-L. Agram¹⁵, J. Andrea, A. Aubin, D. Bloch, J.-M. Brom, M. Buttignol, E.C. Chabert, N. Chanon, C. Collard, E. Conte¹⁵, X. Coubez, J.-C. Fontaine¹⁵, D. Gelé, U. Goerlach, C. Goetzmann, A.-C. Le Bihan, J.A. Merlin², K. Skovpen, P. Van Hove

Centre de Calcul de l'Institut National de Physique Nucleaire et de Physique des Particules, CNRS/IN2P3, Villeurbanne, France

S. Gadrat

Université de Lyon, Université Claude Bernard Lyon 1, CNRS-IN2P3, Institut de Physique Nucléaire de Lyon, Villeurbanne, France

S. Beauceron, C. Bernet, G. Boudoul, E. Bouvier, C.A. Carrillo Montoya, R. Chierici, D. Contardo, B. Courbon, P. Depasse, H. El Mamouni, J. Fan, J. Fay, S. Gascon, M. Gouzevitch, B. Ille, F. Lagarde, I.B. Laktineh, M. Lethuillier, L. Mirabito, A.L. Pequegnot, S. Perries, J.D. Ruiz Alvarez, D. Sabes, V. Sordini, M. Vander Donckt, P. Verdier, S. Viret

Georgian Technical University, Tbilisi, Georgia

T. Toriashvili¹⁶

Tbilisi State University, Tbilisi, Georgia

Z. Tsamalaidze⁹

RWTH Aachen University, I. Physikalisches Institut, Aachen, Germany

C. Autermann, S. Beranek, L. Feld, A. Heister, M.K. Kiesel, K. Klein, M. Lipinski, A. Ostapchuk, M. Preuten, F. Raupach, S. Schael, J.F. Schulte, T. Verlage, H. Weber, V. Zhukov⁵

RWTH Aachen University, III. Physikalisches Institut A, Aachen, Germany

M. Ata, M. Brodski, E. Dietz-Laursonn, D. Duchardt, M. Endres, M. Erdmann, S. Erdweg, T. Esch, R. Fischer, A. Güth, T. Hebbeker, C. Heidemann, K. Hoepfner, S. Knutzen, P. Kreuzer, M. Merschmeyer, A. Meyer, P. Millet, S. Mukherjee, M. Olschewski, K. Padeken, P. Papacz, T. Pook, M. Radziej, H. Reithler, M. Rieger, F. Scheuch, L. Sonnenschein, D. Teyssier, S. Thüer

RWTH Aachen University, III. Physikalisches Institut B, Aachen, Germany

V. Cherepanov, Y. Erdogan, G. Flügge, H. Geenen, M. Geisler, F. Hoehle, B. Kargoll, T. Kress, A. Künsken, J. Lingemann, A. Nehrkorn, A. Nowack, I.M. Nugent, C. Pistone, O. Pooth, A. Stahl

Deutsches Elektronen-Synchrotron, Hamburg, Germany

M. Aldaya Martin, I. Asin, N. Bartosik, O. Behnke, U. Behrens, K. Borras¹⁷, A. Burgmeier, A. Campbell, C. Contreras-Campana, F. Costanza, C. Diez Pardos, G. Dolinska, S. Dooling, T. Dorland, G. Eckerlin, D. Eckstein, T. Eichhorn, G. Flucke, E. Gallo¹⁸, J. Garay Garcia, A. Geiser, A. Gizhko, P. Gunnellini, J. Hauk, M. Hempel¹⁹, H. Jung, A. Kalogeropoulos, O. Karacheban¹⁹, M. Kasemann, P. Katsas, J. Kieseler, C. Kleinwort, I. Korol, W. Lange, J. Leonard, K. Lipka, A. Lobanov, W. Lohmann¹⁹, R. Mankel, I.-A. Melzer-Pellmann,

A.B. Meyer, G. Mittag, J. Mnich, A. Mussgiller, S. Naumann-Emme, A. Nayak, E. Ntomari, H. Perrey, D. Pitzl, R. Placakyte, A. Raspereza, B. Roland, M.Ö. Sahin, P. Saxena, T. Schoerner-Sadenius, C. Seitz, S. Spannagel, N. Stefaniuk, K.D. Trippkewitz, R. Walsh, C. Wissing

University of Hamburg, Hamburg, Germany

V. Blobel, M. Centis Vignali, A.R. Draeger, J. Erfle, E. Garutti, K. Goebel, D. Gonzalez, M. Görner, J. Haller, M. Hoffmann, R.S. Höing, A. Junkes, R. Klanner, R. Kogler, N. Kovalchuk, T. Lapsien, T. Lenz, I. Marchesini, D. Marconi, M. Meyer, D. Nowatschin, J. Ott, F. Pantaleo², T. Peiffer, A. Perieanu, N. Pietsch, J. Poehlsen, C. Sander, C. Scharf, P. Schleper, E. Schlieckau, A. Schmidt, S. Schumann, J. Schwandt, V. Sola, H. Stadie, G. Steinbrück, F.M. Stober, H. Tholen, D. Troendle, E. Usai, L. Vanelderen, A. Vanhoefer, B. Vormwald

Institut für Experimentelle Kernphysik, Karlsruhe, Germany

C. Barth, C. Baus, J. Berger, C. Böser, E. Butz, T. Chwalek, F. Colombo, W. De Boer, A. Descroix, A. Dierlamm, S. Fink, F. Frensch, R. Friese, M. Giffels, A. Gilbert, D. Haitz, F. Hartmann², S.M. Heindl, U. Husemann, I. Katkov⁵, A. Kornmayer², P. Lobelle Pardo, B. Maier, H. Mildner, M.U. Mozer, T. Müller, Th. Müller, M. Plagge, G. Quast, K. Rabbertz, S. Röcker, F. Roscher, M. Schröder, G. Sieber, H.J. Simonis, R. Ulrich, J. Wagner-Kuhr, S. Wayand, M. Weber, T. Weiler, S. Williamson, C. Wöhrmann, R. Wolf

Institute of Nuclear and Particle Physics (INPP), NCSR Demokritos, Aghia Paraskevi, Greece

G. Anagnostou, G. Daskalakis, T. Gerasis, V.A. Giakoumopoulou, A. Kyriakis, D. Loukas, A. Psallidas, I. Topsis-Giotis

National and Kapodistrian University of Athens, Athens, Greece

A. Agapitos, S. Kesisoglou, A. Panagiotou, N. Saoulidou, E. Tziaferi

University of Ioánnina, Ioánnina, Greece

I. Evangelou, G. Flouris, C. Foudas, P. Kokkas, N. Loukas, N. Manthos, I. Papadopoulos, E. Paradas, J. Strologas

Wigner Research Centre for Physics, Budapest, Hungary

G. Bencze, C. Hajdu, A. Hazi, P. Hidas, D. Horvath²⁰, F. Sikler, V. Veszpremi, G. Vesztergombi²¹, A.J. Zsigmond

Institute of Nuclear Research ATOMKI, Debrecen, Hungary

N. Beni, S. Czellar, J. Karancsi²², J. Molnar, Z. Szillasi²

University of Debrecen, Debrecen, Hungary

M. Bartók²³, A. Makovec, P. Raics, Z.L. Trocsanyi, B. Ujvari

National Institute of Science Education and Research, Bhubaneswar, India

S. Choudhury²⁴, P. Mal, K. Mandal, D.K. Sahoo, N. Sahoo, S.K. Swain

Panjab University, Chandigarh, India

S. Bansal, S.B. Beri, V. Bhatnagar, R. Chawla, R. Gupta, U. Bhawandeep, A.K. Kalsi, A. Kaur, M. Kaur, R. Kumar, A. Mehta, M. Mittal, J.B. Singh, G. Walia

University of Delhi, Delhi, India

Ashok Kumar, A. Bhardwaj, B.C. Choudhary, R.B. Garg, S. Malhotra, M. Naimuddin, N. Nishu, K. Ranjan, R. Sharma, V. Sharma

Saha Institute of Nuclear Physics, Kolkata, India

S. Bhattacharya, K. Chatterjee, S. Dey, S. Dutta, N. Majumdar, A. Modak, K. Mondal, S. Mukhopadhyay, A. Roy, D. Roy, S. Roy Chowdhury, S. Sarkar, M. Sharan

Bhabha Atomic Research Centre, Mumbai, India

R. Chudasama, D. Dutta, V. Jha, V. Kumar, A.K. Mohanty², L.M. Pant, P. Shukla, A. Topkar

Tata Institute of Fundamental Research, Mumbai, India

T. Aziz, S. Banerjee, S. Bhowmik²⁵, R.M. Chatterjee, R.K. Dewanjee, S. Dugad, S. Ganguly, S. Ghosh, M. Guchait, A. Gurtu²⁶, Sa. Jain, G. Kole, S. Kumar, B. Mahakud, M. Maity²⁵, G. Majumder, K. Mazumdar, S. Mitra, G.B. Mohanty, B. Parida, T. Sarkar²⁵, N. Sur, B. Sutar, N. Wickramage²⁷

Indian Institute of Science Education and Research (IISER), Pune, India

S. Chauhan, S. Dube, A. Kapoor, K. Kothekar, A. Rane, S. Sharma

Institute for Research in Fundamental Sciences (IPM), Tehran, Iran

H. Bakhshiansohi, H. Behnamian, S.M. Etesami²⁸, A. Fahim²⁹, M. Khakzad, M. Mohammadi Najafabadi, M. Naseri, S. Paktinat Mehdiabadi, F. Rezaei Hosseinabadi, B. Safarzadeh³⁰, M. Zeinali

University College Dublin, Dublin, Ireland

M. Felcini, M. Grunewald

INFN Sezione di Bari ^a, Università di Bari ^b, Politecnico di Bari ^c, Bari, Italy

M. Abbrescia^{a,b}, C. Calabria^{a,b}, C. Caputo^{a,b}, A. Colaleo^a, D. Creanza^{a,c}, L. Cristella^{a,b}, N. De Filippis^{a,c}, M. De Palma^{a,b}, L. Fiore^a, G. Iaselli^{a,c}, G. Maggi^{a,c}, M. Maggi^a, G. Miniello^{a,b}, S. My^{a,c}, S. Nuzzo^{a,b}, A. Pompili^{a,b}, G. Pugliese^{a,c}, R. Radogna^{a,b}, A. Ranieri^a, G. Selvaggi^{a,b}, L. Silvestris^{a,2}, R. Venditti^{a,b}

INFN Sezione di Bologna ^a, Università di Bologna ^b, Bologna, Italy

G. Abbiendi^a, C. Battilana², D. Bonacorsi^{a,b}, S. Braibant-Giacomelli^{a,b}, L. Brigliadori^{a,b}, R. Campanini^{a,b}, P. Capiluppi^{a,b}, A. Castro^{a,b}, F.R. Cavallo^a, S.S. Chhibra^{a,b}, G. Codispoti^{a,b}, M. Cuffiani^{a,b}, G.M. Dallavalle^a, F. Fabbri^a, A. Fanfani^{a,b}, D. Fasanella^{a,b}, P. Giacomelli^a, C. Grandi^a, L. Guiducci^{a,b}, S. Marcellini^a, G. Masetti^a, A. Montanari^a, F.L. Navarria^{a,b}, A. Perrotta^a, A.M. Rossi^{a,b}, T. Rovelli^{a,b}, G.P. Siroli^{a,b}, N. Tosi^{a,b,2}

INFN Sezione di Catania ^a, Università di Catania ^b, Catania, Italy

G. Cappello^b, M. Chiorboli^{a,b}, S. Costa^{a,b}, A. Di Mattia^a, F. Giordano^{a,b}, R. Potenza^{a,b}, A. Tricoli^{a,b}, C. Tuve^{a,b}

INFN Sezione di Firenze ^a, Università di Firenze ^b, Firenze, Italy

G. Barbagli^a, V. Ciulli^{a,b}, C. Civinini^a, R. D'Alessandro^{a,b}, E. Focardi^{a,b}, V. Gori^{a,b}, P. Lenzi^{a,b}, M. Meschini^a, S. Paoletti^a, G. Sguazzoni^a, L. Viliani^{a,b,2}

INFN Laboratori Nazionali di Frascati, Frascati, Italy

L. Benussi, S. Bianco, F. Fabbri, D. Piccolo, F. Primavera²

INFN Sezione di Genova ^a, Università di Genova ^b, Genova, Italy

V. Calvelli^{a,b}, F. Ferro^a, M. Lo Vetere^{a,b}, M.R. Monge^{a,b}, E. Robutti^a, S. Tosi^{a,b}

INFN Sezione di Milano-Bicocca ^a, Università di Milano-Bicocca ^b, Milano, Italy

L. Brianza, M.E. Dinardo^{a,b}, S. Fiorendi^{a,b}, S. Gennai^a, R. Gerosa^{a,b}, A. Ghezzi^{a,b}, P. Govoni^{a,b}, S. Malvezzi^a, R.A. Manzoni^{a,b,2}, B. Marzocchi^{a,b}, D. Menasce^a, L. Moroni^a, M. Paganoni^{a,b}, D. Pedrini^a, S. Ragazzi^{a,b}, N. Redaelli^a, T. Tabarelli de Fatis^{a,b}

INFN Sezione di Napoli ^a, Università di Napoli 'Federico II' ^b, Napoli, Italy, Università della Basilicata ^c, Potenza, Italy, Università G. Marconi ^d, Roma, Italy

S. Buontempo^a, N. Cavallo^{a,c}, S. Di Guida^{a,d,2}, M. Esposito^{a,b}, F. Fabozzi^{a,c}, A.O.M. Iorio^{a,b}, G. Lanza^a, L. Lista^a, S. Meola^{a,d,2}, M. Merola^a, P. Paolucci^{a,2}, C. Sciacca^{a,b}, F. Thyssen

INFN Sezione di Padova ^a, Università di Padova ^b, Padova, Italy, Università di Trento ^c, Trento, Italy

P. Azzi^{a,2}, N. Bacchetta^a, L. Benato^{a,b}, D. Bisello^{a,b}, A. Boletti^{a,b}, A. Branca^{a,b}, R. Carlin^{a,b}, P. Checchia^a, M. Dall'Osso^{a,b,2}, T. Dorigo^a, U. Dosselli^a, F. Fanzago^a, U. Gasparini^{a,b}, F. Gonella^a, A. Gozzelino^a, K. Kanishchev^{a,c}, S. Lacaprara^a, M. Margoni^{a,b}, G. Maron^{a,31}, A.T. Meneguzzo^{a,b}, J. Pazzini^{a,b,2}, N. Pozzobon^{a,b}, P. Ronchese^{a,b}, F. Simonetto^{a,b}, E. Torassa^a, M. Tosi^{a,b}, M. Zanetti, P. Zotto^{a,b}, A. Zucchetta^{a,b,2}

INFN Sezione di Pavia ^a, Università di Pavia ^b, Pavia, Italy

A. Braghieri^a, A. Magnani^{a,b}, P. Montagna^{a,b}, S.P. Ratti^{a,b}, V. Re^a, C. Riccardi^{a,b}, P. Salvini^a, I. Vai^{a,b}, P. Vitulo^{a,b}

INFN Sezione di Perugia ^a, Università di Perugia ^b, Perugia, Italy

L. Alunni Solestizi^{a,b}, G.M. Bilei^a, D. Ciangottini^{a,b}, L. Fano^{a,b}, P. Lariccia^{a,b}, G. Mantovani^{a,b}, M. Menichelli^a, A. Saha^a, A. Santocchia^{a,b}

INFN Sezione di Pisa ^a, Università di Pisa ^b, Scuola Normale Superiore di Pisa ^c, Pisa, Italy

K. Androsov^{a,32}, P. Azzurri^{a,2}, G. Bagliesi^a, J. Bernardini^a, T. Boccali^a, R. Castaldi^a, M.A. Ciocci^{a,32}, R. Dell'Orso^a, S. Donato^{a,c}, G. Fedi, L. Foà^{a,c†}, A. Giassi^a, M.T. Grippo^{a,32}, E. Ligabue^{a,c}, T. Lomtadze^a, L. Martini^{a,b}, A. Messineo^{a,b}, F. Palla^a, A. Rizzi^{a,b}, A. Savoy-Navarro^{a,33}, P. Spagnolo^a, R. Tenchini^a, G. Tonelli^{a,b}, A. Venturi^a, P.G. Verdini^a

INFN Sezione di Roma ^a, Università di Roma ^b, Roma, Italy

L. Barone^{a,b}, F. Cavallari^a, G. D'imperio^{a,b,2}, D. Del Re^{a,b,2}, M. Diemoz^a, S. Gelli^{a,b}, C. Jorda^a, E. Longo^{a,b}, F. Margaroli^{a,b}, P. Meridiani^a, G. Organtini^{a,b}, R. Paramatti^a, F. Preiato^{a,b}, S. Rahatlou^{a,b}, C. Rovelli^a, F. Santanastasio^{a,b}

INFN Sezione di Torino ^a, Università di Torino ^b, Torino, Italy, Università del Piemonte Orientale ^c, Novara, Italy

N. Amapane^{a,b}, R. Arcidiacono^{a,c,2}, S. Argiro^{a,b}, M. Arneodo^{a,c}, R. Bellan^{a,b}, C. Biino^a, N. Cartiglia^a, M. Costa^{a,b}, R. Covarelli^{a,b}, A. Degano^{a,b}, N. Demaria^a, L. Finco^{a,b}, B. Kiani^{a,b}, C. Mariotti^a, S. Maselli^a, E. Migliore^{a,b}, V. Monaco^{a,b}, E. Monteil^{a,b}, M.M. Obertino^{a,b}, L. Pacher^{a,b}, N. Pastrone^a, M. Pelliccioni^a, G.L. Pinna Angioni^{a,b}, F. Ravera^{a,b}, A. Romero^{a,b}, M. Ruspa^{a,c}, R. Sacchi^{a,b}, A. Solano^{a,b}, A. Staiano^a

INFN Sezione di Trieste ^a, Università di Trieste ^b, Trieste, Italy

S. Belforte^a, V. Candelise^{a,b}, M. Casarsa^a, F. Cossutti^a, G. Della Ricca^{a,b}, B. Gobbo^a, C. La Licata^{a,b}, M. Marone^{a,b}, A. Schizzi^{a,b}, A. Zanetti^a

Kangwon National University, Chunchon, Korea

A. Kropivnitskaya, S.K. Nam

Kyungpook National University, Daegu, Korea

D.H. Kim, G.N. Kim, M.S. Kim, D.J. Kong, S. Lee, Y.D. Oh, A. Sakharov, D.C. Son

Chonbuk National University, Jeonju, Korea

J.A. Brochero Cifuentes, H. Kim, T.J. Kim³⁴

Chonnam National University, Institute for Universe and Elementary Particles, Kwangju, Korea

S. Song

Korea University, Seoul, Korea

S. Cho, S. Choi, Y. Go, D. Gyun, B. Hong, H. Kim, Y. Kim, B. Lee, K. Lee, K.S. Lee, S. Lee, J. Lim, S.K. Park, Y. Roh

Seoul National University, Seoul, Korea

H.D. Yoo

University of Seoul, Seoul, Korea

M. Choi, H. Kim, J.H. Kim, J.S.H. Lee, I.C. Park, G. Ryu, M.S. Ryu

Sungkyunkwan University, Suwon, Korea

Y. Choi, J. Goh, D. Kim, E. Kwon, J. Lee, I. Yu

Vilnius University, Vilnius, Lithuania

V. Dudenas, A. Juodagalvis, J. Vaitkus

National Centre for Particle Physics, Universiti Malaya, Kuala Lumpur, Malaysia

I. Ahmed, Z.A. Ibrahim, J.R. Komaragiri, M.A.B. Md Ali³⁵, F. Mohamad Idris³⁶, W.A.T. Wan Abdullah, M.N. Yusli, Z. Zolkapli

Centro de Investigacion y de Estudios Avanzados del IPN, Mexico City, Mexico

E. Casimiro Linares, H. Castilla-Valdez, E. De La Cruz-Burelo, I. Heredia-De La Cruz³⁷, A. Hernandez-Almada, R. Lopez-Fernandez, J. Mejia Guisao, A. Sanchez-Hernandez

Universidad Iberoamericana, Mexico City, Mexico

S. Carrillo Moreno, F. Vazquez Valencia

Benemerita Universidad Autonoma de Puebla, Puebla, Mexico

I. Pedraza, H.A. Salazar Ibarguen

Universidad Autónoma de San Luis Potosí, San Luis Potosí, Mexico

A. Morelos Pineda

University of Auckland, Auckland, New Zealand

D. Krofcheck

University of Canterbury, Christchurch, New Zealand

P.H. Butler

National Centre for Physics, Quaid-I-Azam University, Islamabad, Pakistan

A. Ahmad, M. Ahmad, Q. Hassan, H.R. Hoorani, W.A. Khan, T. Khurshid, M. Shoaib, M. Waqas

National Centre for Nuclear Research, Swierk, Poland

H. Bialkowska, M. Bluj, B. Boimska, T. Frueboes, M. Górski, M. Kazana, K. Nawrocki, K. Romanowska-Rybinska, M. Szleper, P. Traczyk, P. Zalewski

Institute of Experimental Physics, Faculty of Physics, University of Warsaw, Warsaw, Poland

G. Brona, K. Bunkowski, A. Byszuk³⁸, K. Doroba, A. Kalinowski, M. Konecki, J. Krolikowski, M. Misiura, M. Olszewski, M. Walczak

Laboratório de Instrumentação e Física Experimental de Partículas, Lisboa, Portugal

P. Bargassa, C. Beirão Da Cruz E Silva, A. Di Francesco, P. Faccioli, P.G. Ferreira Parracho,

M. Gallinaro, J. Hollar, N. Leonardo, L. Lloret Iglesias, F. Nguyen, J. Rodrigues Antunes, J. Seixas, O. Toldaiev, D. Vadrucchio, J. Varela, P. Vischia

Joint Institute for Nuclear Research, Dubna, Russia

S. Afanasiev, P. Bunin, M. Gavrilenko, I. Golutvin, I. Gorbunov, A. Kamenev, V. Karjavin, A. Lanev, A. Malakhov, V. Matveev^{39,40}, P. Moiseenz, V. Palichik, V. Perelygin, S. Shmatov, S. Shulha, N. Skatchkov, V. Smirnov, A. Zarubin

Petersburg Nuclear Physics Institute, Gatchina (St. Petersburg), Russia

V. Golovtsov, Y. Ivanov, V. Kim⁴¹, E. Kuznetsova, P. Levchenko, V. Murzin, V. Oreshkin, I. Smirnov, V. Sulimov, L. Uvarov, S. Vavilov, A. Vorobyev

Institute for Nuclear Research, Moscow, Russia

Yu. Andreev, A. Dermenev, S. Gninenko, N. Golubev, A. Karneyeu, M. Kirsanov, N. Krasnikov, A. Pashenkov, D. Tlisov, A. Toropin

Institute for Theoretical and Experimental Physics, Moscow, Russia

V. Epshteyn, V. Gavrillov, N. Lychkovskaya, V. Popov, I. Pozdnyakov, G. Safronov, A. Spiridonov, E. Vlasov, A. Zhokin

National Research Nuclear University 'Moscow Engineering Physics Institute' (MEPhI), Moscow, Russia

M. Chadeeva, R. Chistov, M. Danilov, V. Rusinov, E. Tarkovskii

P.N. Lebedev Physical Institute, Moscow, Russia

V. Andreev, M. Azarkin⁴⁰, I. Dremin⁴⁰, M. Kirakosyan, A. Leonidov⁴⁰, G. Mesyats, S.V. Rusakov

Skobeltsyn Institute of Nuclear Physics, Lomonosov Moscow State University, Moscow, Russia

A. Baskakov, A. Belyaev, E. Boos, A. Ershov, A. Gribushin, L. Khein, V. Klyukhin, O. Kodolova, I. Lokhtin, O. Lukina, I. Miagkov, S. Obraztsov, S. Petrushanko, V. Savrin, A. Snigirev

State Research Center of Russian Federation, Institute for High Energy Physics, Protvino, Russia

I. Azhgirey, I. Bayshev, S. Bitioukov, V. Kachanov, A. Kalinin, D. Konstantinov, V. Krychkin, V. Petrov, R. Ryutin, A. Sobol, L. Tourtchanovitch, S. Troshin, N. Tyurin, A. Uzunian, A. Volkov

University of Belgrade, Faculty of Physics and Vinca Institute of Nuclear Sciences, Belgrade, Serbia

P. Adzic⁴², P. Cirkovic, D. Devetak, J. Milosevic, V. Rekovic

Centro de Investigaciones Energéticas Medioambientales y Tecnológicas (CIEMAT), Madrid, Spain

J. Alcaraz Maestre, E. Calvo, M. Cerrada, M. Chamizo Llatas, N. Colino, B. De La Cruz, A. Delgado Peris, A. Escalante Del Valle, C. Fernandez Bedoya, J.P. Fernández Ramos, J. Flix, M.C. Fouz, P. Garcia-Abia, O. Gonzalez Lopez, S. Goy Lopez, J.M. Hernandez, M.I. Josa, E. Navarro De Martino, A. Pérez-Calero Yzquierdo, J. Puerta Pelayo, A. Quintario Olmeda, I. Redondo, L. Romero, M.S. Soares

Universidad Autónoma de Madrid, Madrid, Spain

C. Albajar, J.F. de Trocóniz, M. Missiroli, D. Moran

Universidad de Oviedo, Oviedo, Spain

J. Cuevas, J. Fernandez Menendez, S. Folgueras, I. Gonzalez Caballero, E. Palencia Cortezon, J.M. Vizan Garcia

Instituto de Física de Cantabria (IFCA), CSIC-Universidad de Cantabria, Santander, Spain

I.J. Cabrillo, A. Calderon, J.R. Castiñeiras De Saa, E. Curras, P. De Castro Manzano, M. Fernandez, J. Garcia-Ferrero, G. Gomez, A. Lopez Virto, J. Marco, R. Marco, C. Martinez Rivero, F. Matorras, J. Piedra Gomez, T. Rodrigo, A.Y. Rodríguez-Marrero, A. Ruiz-Jimeno, L. Scodellaro, N. Trevisani, I. Vila, R. Vilar Cortabitarte

CERN, European Organization for Nuclear Research, Geneva, Switzerland

D. Abbaneo, E. Auffray, G. Auzinger, M. Bachtis, P. Baillon, A.H. Ball, D. Barney, A. Benaglia, J. Bendavid, L. Benhabib, G.M. Berruti, P. Bloch, A. Bocci, A. Bonato, C. Botta, H. Breuker, T. Camporesi, R. Castello, M. Cepeda, G. Cerminara, M. D'Alfonso, D. d'Enterria, A. Dabrowski, V. Daponte, A. David, M. De Gruttola, F. De Guio, A. De Roeck, E. Di Marco⁴³, M. Dobson, M. Dordevic, B. Dorney, T. du Pree, D. Duggan, M. Dünser, N. Dupont, A. Elliott-Peisert, G. Franzoni, J. Fulcher, W. Funk, D. Gigi, K. Gill, D. Giordano, M. Girone, F. Glege, R. Guida, S. Gundacker, M. Guthoff, J. Hammer, P. Harris, J. Hegeman, V. Innocente, P. Janot, H. Kirschenmann, M.J. Kortelainen, K. Kousouris, P. Lecoq, C. Lourenço, M.T. Lucchini, N. Magini, L. Malgeri, M. Mannelli, A. Martelli, L. Masetti, F. Meijers, S. Mersi, E. Meschi, F. Moortgat, S. Morovic, M. Mulders, M.V. Nemallapudi, H. Neugebauer, S. Orfanelli⁴⁴, L. Orsini, L. Pape, E. Perez, M. Peruzzi, A. Petrilli, G. Petrucciani, A. Pfeiffer, M. Pierini, D. Piparo, A. Racz, T. Reis, G. Rolandi⁴⁵, M. Rovere, M. Ruan, H. Sakulin, C. Schäfer, C. Schwick, M. Seidel, A. Sharma, P. Silva, M. Simon, P. Sphicas⁴⁶, J. Steggemann, B. Stieger, M. Stoye, Y. Takahashi, D. Treille, A. Triossi, A. Tsiros, G.I. Veres⁴⁷, N. Wardle, H.K. Wöhri, A. Zagozdzińska³⁸, W.D. Zeuner

Paul Scherrer Institut, Villigen, Switzerland

W. Bertl, K. Deiters, W. Erdmann, R. Horisberger, Q. Ingram, H.C. Kaestli, D. Kotlinski, U. Langenegger, T. Rohe

Institute for Particle Physics, ETH Zurich, Zurich, Switzerland

F. Bachmair, L. Bäni, L. Bianchini, B. Casal, G. Dissertori, M. Dittmar, M. Donegà, P. Eller, C. Grab, C. Heidegger, D. Hits, J. Hoss, G. Kasieczka, P. Lecomte[†], W. Lustermann, B. Mangano, M. Marionneau, P. Martinez Ruiz del Arbol, M. Masciovecchio, M.T. Meinhard, D. Meister, F. Micheli, P. Musella, F. Nessi-Tedaldi, F. Pandolfi, J. Pata, F. Pauss, G. Perrin, L. Perrozzi, M. Quittnat, M. Rossini, M. Schönenberger, A. Starodumov⁴⁸, M. Takahashi, V.R. Tavolaro, K. Theofilatos, R. Wallny

Universität Zürich, Zurich, Switzerland

T.K. Aarrestad, C. AMSLER⁴⁹, L. Caminada, M.F. Canelli, V. Chiochia, A. De Cosa, C. Galloni, A. Hinzmann, T. Hreus, B. Kilminster, C. Lange, J. Ngadiuba, D. Pinna, G. Rauco, P. Robmann, D. Salerno, Y. Yang

National Central University, Chung-Li, Taiwan

K.H. Chen, T.H. Doan, Sh. Jain, R. Khurana, M. Konyushikhin, C.M. Kuo, W. Lin, Y.J. Lu, A. Pozdnyakov, S.S. Yu

National Taiwan University (NTU), Taipei, Taiwan

Arun Kumar, P. Chang, Y.H. Chang, Y.W. Chang, Y. Chao, K.F. Chen, P.H. Chen, C. Dietz, F. Fiori, U. Grundler, W.-S. Hou, Y. Hsiung, Y.F. Liu, R.-S. Lu, M. Miñano Moya, E. Petrakou, J.f. Tsai, Y.M. Tzeng

Chulalongkorn University, Faculty of Science, Department of Physics, Bangkok, Thailand

B. Asavapibhop, K. Kovitangoon, G. Singh, N. Srimanobhas, N. Suwonjandee

Cukurova University, Adana, Turkey

A. Adiguzel, S. Damarseckin, Z.S. Demiroglu, C. Dozen, I. Dumanoglu, S. Girgis, G. Gokbulut, Y. Guler, E. Gurpinar, I. Hos, E.E. Kangal⁵⁰, A. Kayis Topaksu, G. Onengut⁵¹, K. Ozdemir⁵², S. Ozturk⁵³, D. Sunar Cerci⁵⁴, B. Tali⁵⁴, H. Topakli⁵³, C. Zorbilmez

Middle East Technical University, Physics Department, Ankara, Turkey

B. Bilin, S. Bilmis, B. Isildak⁵⁵, G. Karapinar⁵⁶, M. Yalvac, M. Zeyrek

Bogazici University, Istanbul, Turkey

E. Gülmez, M. Kaya⁵⁷, O. Kaya⁵⁸, E.A. Yetkin⁵⁹, T. Yetkin⁶⁰

Istanbul Technical University, Istanbul, Turkey

A. Cakir, K. Cankocak, S. Sen⁶¹, F.I. Vardarli

Institute for Scintillation Materials of National Academy of Science of Ukraine, Kharkov, Ukraine

B. Grynyov

National Scientific Center, Kharkov Institute of Physics and Technology, Kharkov, Ukraine

L. Levchuk, P. Sorokin

University of Bristol, Bristol, United Kingdom

R. Aggleton, F. Ball, L. Beck, J.J. Brooke, D. Burns, E. Clement, D. Cussans, H. Flacher, J. Goldstein, M. Grimes, G.P. Heath, H.F. Heath, J. Jacob, L. Kreczko, C. Lucas, Z. Meng, D.M. Newbold⁶², S. Paramesvaran, A. Poll, T. Sakuma, S. Seif El Nasr-storey, S. Senkin, D. Smith, V.J. Smith

Rutherford Appleton Laboratory, Didcot, United Kingdom

K.W. Bell, A. Belyaev⁶³, C. Brew, R.M. Brown, L. Calligaris, D. Cieri, D.J.A. Cockerill, J.A. Coughlan, K. Harder, S. Harper, E. Olaiya, D. Petyt, C.H. Shepherd-Themistocleous, A. Thea, I.R. Tomalin, T. Williams, S.D. Worm

Imperial College, London, United Kingdom

M. Baber, R. Bainbridge, O. Buchmuller, A. Bundock, D. Burton, S. Casasso, M. Citron, D. Colling, L. Corpe, P. Dauncey, G. Davies, A. De Wit, M. Della Negra, P. Dunne, A. Elwood, D. Futyan, G. Hall, G. Iles, R. Lane, R. Lucas⁶², L. Lyons, A.-M. Magnan, S. Malik, J. Nash, A. Nikitenko⁴⁸, J. Pela, M. Pesaresi, D.M. Raymond, A. Richards, A. Rose, C. Seez, A. Tapper, K. Uchida, M. Vazquez Acosta⁶⁴, T. Virdee, S.C. Zenz

Brunel University, Uxbridge, United Kingdom

J.E. Cole, P.R. Hobson, A. Khan, P. Kyberd, D. Leslie, I.D. Reid, P. Symonds, L. Teodorescu, M. Turner

Baylor University, Waco, USA

A. Borzou, K. Call, J. Dittmann, K. Hatakeyama, H. Liu, N. Pastika

The University of Alabama, Tuscaloosa, USA

O. Charaf, S.I. Cooper, C. Henderson, P. Rumerio

Boston University, Boston, USA

D. Arcaro, A. Avetisyan, T. Bose, D. Gastler, D. Rankin, C. Richardson, J. Rohlf, L. Sulak, D. Zou

Brown University, Providence, USA

J. Alimena, G. Benelli, E. Berry, D. Cutts, A. Ferapontov, A. Garabedian, J. Hakala, U. Heintz, O. Jesus, E. Laird, G. Landsberg, Z. Mao, M. Narain, S. Piperov, S. Sagir, R. Syarif

University of California, Davis, Davis, USA

R. Breedon, G. Breto, M. Calderon De La Barca Sanchez, S. Chauhan, M. Chertok, J. Conway, R. Conway, P.T. Cox, R. Erbacher, G. Funk, M. Gardner, W. Ko, R. Lander, C. Mclean, M. Mulhearn, D. Pellett, J. Pilot, F. Ricci-Tam, S. Shalhout, J. Smith, M. Squires, D. Stolp, M. Tripathi, S. Wilbur, R. Yohay

University of California, Los Angeles, USA

R. Cousins, P. Everaerts, A. Florent, J. Hauser, M. Ignatenko, D. Saltzberg, E. Takasugi, V. Valuev, M. Weber

University of California, Riverside, Riverside, USA

K. Burt, R. Clare, J. Ellison, J.W. Gary, G. Hanson, J. Heilman, M. Ivova PANEVA, P. Jandir, E. Kennedy, F. Lacroix, O.R. Long, M. Malberti, M. Olmedo Negrete, A. Shrinivas, H. Wei, S. Wimpenny, B. R. Yates

University of California, San Diego, La Jolla, USA

J.G. Branson, G.B. Cerati, S. Cittolin, R.T. D'Agnolo, M. Derdzinski, A. Holzner, R. Kelley, D. Klein, J. Letts, I. Macneill, D. Olivito, S. Padhi, M. Pieri, M. Sani, V. Sharma, S. Simon, M. Tadel, A. Vartak, S. Wasserbaech⁶⁵, C. Welke, F. Würthwein, A. Yagil, G. Zevi Della Porta

University of California, Santa Barbara, Santa Barbara, USA

J. Bradmiller-Feld, C. Campagnari, A. Dishaw, V. Dutta, K. Flowers, M. Franco Sevilla, P. Geffert, C. George, F. Golf, L. Gouskos, J. Gran, J. Incandela, N. Mccoll, S.D. Mullin, J. Richman, D. Stuart, I. Suarez, C. West, J. Yoo

California Institute of Technology, Pasadena, USA

D. Anderson, A. Apresyan, A. Bornheim, J. Bunn, Y. Chen, J. Duarte, A. Mott, H.B. Newman, C. Pena, M. Spiropulu, J.R. Vlimant, S. Xie, R.Y. Zhu

Carnegie Mellon University, Pittsburgh, USA

M.B. Andrews, V. Azzolini, A. Calamba, B. Carlson, T. Ferguson, M. Paulini, J. Russ, M. Sun, H. Vogel, I. Vorobiev

University of Colorado Boulder, Boulder, USA

J.P. Cumalat, W.T. Ford, A. Gaz, F. Jensen, A. Johnson, M. Krohn, T. Mulholland, U. Nauenberg, K. Stenson, S.R. Wagner

Cornell University, Ithaca, USA

J. Alexander, A. Chatterjee, J. Chaves, J. Chu, S. Dittmer, N. Eggert, N. Mirman, G. Nicolas Kaufman, J.R. Patterson, A. Rinkevicius, A. Ryd, L. Skinnari, L. Soffi, W. Sun, S.M. Tan, W.D. Teo, J. Thom, J. Thompson, J. Tucker, Y. Weng, P. Wittich

Fermi National Accelerator Laboratory, Batavia, USA

S. Abdullin, M. Albrow, G. Apollinari, S. Banerjee, L.A.T. Bauerdick, A. Beretvas, J. Berryhill, P.C. Bhat, G. Bolla, K. Burkett, J.N. Butler, H.W.K. Cheung, F. Chlebana, S. Cihangir, V.D. Elvira, I. Fisk, J. Freeman, E. Gottschalk, L. Gray, D. Green, S. Grünendahl, O. Gutsche, J. Hanlon, D. Hare, R.M. Harris, S. Hasegawa, J. Hirschauer, Z. Hu, B. Jayatilaka, S. Jindariani, M. Johnson, U. Joshi, B. Klima, B. Kreis, S. Lammel, J. Lewis, J. Linacre, D. Lincoln, R. Lipton, T. Liu, R. Lopes De Sá, J. Lykken, K. Maeshima, J.M. Marraffino, S. Maruyama, D. Mason, P. McBride, P. Merkel, S. Mrenna, S. Nahn, C. Newman-Holmes[†], V. O'Dell, K. Pedro, O. Prokofyev, G. Rakness, E. Sexton-Kennedy, A. Soha, W.J. Spalding, L. Spiegel, S. Stoynev, N. Strobbe, L. Taylor, S. Tkaczyk, N.V. Tran, L. Uplegger, E.W. Vaandering, C. Vernieri, M. Verzocchi, R. Vidal, M. Wang, H.A. Weber, A. Whitbeck

University of Florida, Gainesville, USA

D. Acosta, P. Avery, P. Bortignon, D. Bourilkov, A. Brinkerhoff, A. Carnes, M. Carver, D. Curry, S. Das, R.D. Field, I.K. Furic, J. Konigsberg, A. Korytov, K. Kotov, P. Ma, K. Matchev, H. Mei, P. Milenovic⁶⁶, G. Mitselmakher, D. Rank, R. Rossin, L. Shchutska, M. Snowball, D. Sperka, N. Terentyev, L. Thomas, J. Wang, S. Wang, J. Yelton

Florida International University, Miami, USA

S. Linn, P. Markowitz, G. Martinez, J.L. Rodriguez

Florida State University, Tallahassee, USA

A. Ackert, J.R. Adams, T. Adams, A. Askew, S. Bein, J. Bochenek, B. Diamond, J. Haas, S. Hagopian, V. Hagopian, K.F. Johnson, A. Khatiwada, H. Prosper, M. Weinberg

Florida Institute of Technology, Melbourne, USA

M.M. Baarmand, V. Bhopatkar, S. Colafranceschi⁶⁷, M. Hohlmann, H. Kalakhety, D. Noonan, T. Roy, F. Yumiceva

University of Illinois at Chicago (UIC), Chicago, USA

M.R. Adams, L. Apanasevich, D. Berry, R.R. Betts, I. Bucinskaite, R. Cavanaugh, O. Evdokimov, L. Gauthier, C.E. Gerber, D.J. Hofman, P. Kurt, C. O'Brien, I.D. Sandoval Gonzalez, P. Turner, N. Varelas, Z. Wu, M. Zakaria, J. Zhang

The University of Iowa, Iowa City, USA

B. Bilki⁶⁸, W. Clarida, K. Dilsiz, S. Durgut, R.P. Gandrajula, M. Haytmyradov, V. Khristenko, J.-P. Merlo, H. Mermerkaya⁶⁹, A. Mestvirishvili, A. Moeller, J. Nachtman, H. Ogul, Y. Onel, F. Ozok⁷⁰, A. Penzo, C. Snyder, E. Tiras, J. Wetzel, K. Yi

Johns Hopkins University, Baltimore, USA

I. Anderson, B.A. Barnett, B. Blumenfeld, A. Cocoros, N. Eminizer, D. Fehling, L. Feng, A.V. Gritsan, P. Maksimovic, M. Osherson, J. Roskes, U. Sarica, M. Swartz, M. Xiao, Y. Xin, C. You

The University of Kansas, Lawrence, USA

P. Baringer, A. Bean, C. Bruner, R.P. Kenny III, D. Majumder, M. Malek, W. Mcbrayer, M. Murray, S. Sanders, R. Stringer, Q. Wang

Kansas State University, Manhattan, USA

A. Ivanov, K. Kaadze, S. Khalil, M. Makouski, Y. Maravin, A. Mohammadi, L.K. Saini, N. Skhirtladze, S. Toda

Lawrence Livermore National Laboratory, Livermore, USA

D. Lange, F. Rebassoo, D. Wright

University of Maryland, College Park, USA

C. Anelli, A. Baden, O. Baron, A. Belloni, B. Calvert, S.C. Eno, C. Ferraioli, J.A. Gomez, N.J. Hadley, S. Jabeen, R.G. Kellogg, T. Kolberg, J. Kunkle, Y. Lu, A.C. Mignerey, Y.H. Shin, A. Skuja, M.B. Tonjes, S.C. Tonwar

Massachusetts Institute of Technology, Cambridge, USA

A. Apyan, R. Barbieri, A. Baty, R. Bi, K. Bierwagen, S. Brandt, W. Busza, I.A. Cali, Z. Demiragli, L. Di Matteo, G. Gomez Ceballos, M. Goncharov, D. Gulhan, Y. Iiyama, G.M. Innocenti, M. Klute, D. Kovalskyi, K. Krajczar, Y.S. Lai, Y.-J. Lee, A. Levin, P.D. Luckey, A.C. Marini, C. McGinn, C. Mironov, S. Narayanan, X. Niu, C. Paus, C. Roland, G. Roland, J. Salfeld-Nebgen, G.S.F. Stephens, K. Sumorok, K. Tatar, M. Varma, D. Velicanu, J. Veverka, J. Wang, T.W. Wang, B. Wyslouch, M. Yang, V. Zhukova

University of Minnesota, Minneapolis, USA

A.C. Benvenuti, B. Dahmes, A. Evans, A. Finkel, A. Gude, P. Hansen, S. Kalafut, S.C. Kao, K. Klapoetke, Y. Kubota, Z. Lesko, J. Mans, S. Nourbakhsh, N. Ruckstuhl, R. Rusack, N. Tambe, J. Turkewitz

University of Mississippi, Oxford, USA

J.G. Acosta, S. Oliveros

University of Nebraska-Lincoln, Lincoln, USA

E. Avdeeva, R. Bartek, K. Bloom, S. Bose, D.R. Claes, A. Dominguez, C. Fangmeier, R. Gonzalez Suarez, R. Kamalieddin, D. Knowlton, I. Kravchenko, F. Meier, J. Monroy, F. Ratnikov, J.E. Siado, G.R. Snow

State University of New York at Buffalo, Buffalo, USA

M. Alyari, J. Dolen, J. George, A. Godshalk, C. Harrington, I. Iashvili, J. Kaisen, A. Kharchilava, A. Kumar, S. Rappoccio, B. Roozbahani

Northeastern University, Boston, USA

G. Alverson, E. Barberis, D. Baumgartel, M. Chasco, A. Hortiangtham, A. Massironi, D.M. Morse, D. Nash, T. Orimoto, R. Teixeira De Lima, D. Trocino, R.-J. Wang, D. Wood, J. Zhang

Northwestern University, Evanston, USA

S. Bhattacharya, K.A. Hahn, A. Kubik, J.F. Low, N. Mucia, N. Odell, B. Pollack, M. Schmitt, K. Sung, M. Trovato, M. Velasco

University of Notre Dame, Notre Dame, USA

N. Dev, M. Hildreth, C. Jessop, D.J. Karmgard, N. Kellams, K. Lannon, N. Marinelli, F. Meng, C. Mueller, Y. Musienko³⁹, M. Planer, A. Reinsvold, R. Ruchti, N. Rupprecht, G. Smith, S. Taroni, N. Valls, M. Wayne, M. Wolf, A. Woodard

The Ohio State University, Columbus, USA

L. Antonelli, J. Brinson, B. Bylsma, L.S. Durkin, S. Flowers, A. Hart, C. Hill, R. Hughes, W. Ji, T.Y. Ling, B. Liu, W. Luo, D. Puigh, M. Rodenburg, B.L. Winer, H.W. Wulsin

Princeton University, Princeton, USA

O. Driga, P. Elmer, J. Hardenbrook, P. Hebda, S.A. Koay, P. Lujan, D. Marlow, T. Medvedeva, M. Mooney, J. Olsen, C. Palmer, P. Piroué, D. Stickland, C. Tully, A. Zuranski

University of Puerto Rico, Mayaguez, USA

S. Malik

Purdue University, West Lafayette, USA

A. Barker, V.E. Barnes, D. Benedetti, D. Bortoletto, L. Gutay, M.K. Jha, M. Jones, A.W. Jung, K. Jung, A. Kumar, D.H. Miller, N. Neumeister, B.C. Radburn-Smith, X. Shi, I. Shipsey, D. Silvers, J. Sun, A. Svyatkovskiy, F. Wang, W. Xie, L. Xu

Purdue University Calumet, Hammond, USA

N. Parashar, J. Stupak

Rice University, Houston, USA

A. Adair, B. Akgun, Z. Chen, K.M. Ecklund, F.J.M. Geurts, M. Guilbaud, W. Li, B. Michlin, M. Northup, B.P. Padley, R. Redjimi, J. Roberts, J. Rorie, Z. Tu, J. Zabel

University of Rochester, Rochester, USA

B. Betchart, A. Bodek, P. de Barbaro, R. Demina, Y. Eshaq, T. Ferbel, M. Galanti, A. Garcia-Bellido, J. Han, O. Hindrichs, A. Khukhunaishvili, K.H. Lo, P. Tan, M. Verzetti

The Rockefeller University, New York, USA

R. Ciesielski

Rutgers, The State University of New Jersey, Piscataway, USA

J.P. Chou, E. Contreras-Campana, D. Ferencek, Y. Gershtein, E. Halkiadakis, M. Heindl, D. Hidas, E. Hughes, S. Kaplan, R. Kunnawalkam Elayavalli, A. Lath, K. Nash, H. Saka, S. Salur, S. Schnetzer, D. Sheffield, S. Somalwar, R. Stone, S. Thomas, P. Thomassen, M. Walker

University of Tennessee, Knoxville, USA

M. Foerster, G. Riley, K. Rose, S. Spanier, K. Thapa

Texas A&M University, College Station, USA

O. Bouhali⁷¹, A. Castaneda Hernandez⁷¹, A. Celik, M. Dalchenko, M. De Mattia, A. Delgado, S. Dildick, R. Eusebi, J. Gilmore, T. Huang, T. Kamon⁷², V. Krutelyov, R. Mueller, I. Osipenkov, Y. Pakhotin, R. Patel, A. Perloff, D. Rathjens, A. Rose, A. Safonov, A. Tatarinov, K.A. Ulmer

Texas Tech University, Lubbock, USA

N. Akchurin, C. Cowden, J. Damgov, C. Dragoiu, P.R. Duerdo, J. Faulkner, S. Kunori, K. Lamichhane, S.W. Lee, T. Libeiro, S. Undleeb, I. Volobouev

Vanderbilt University, Nashville, USA

E. Appelt, A.G. Delannoy, S. Greene, A. Gurrola, R. Janjam, W. Johns, C. Maguire, Y. Mao, A. Melo, H. Ni, P. Sheldon, S. Tuo, J. Velkovska, Q. Xu

University of Virginia, Charlottesville, USA

M.W. Arenton, B. Cox, B. Francis, J. Goodell, R. Hirosky, A. Ledovskoy, H. Li, C. Neu, T. Sinthuprasith, X. Sun, Y. Wang, E. Wolfe, J. Wood, F. Xia

Wayne State University, Detroit, USA

C. Clarke, R. Harr, P.E. Karchin, C. Kottachchi Kankanamge Don, P. Lamichhane, J. Sturdy

University of Wisconsin - Madison, Madison, WI, USA

D.A. Belknap, D. Carlsmith, S. Dasu, L. Dodd, S. Duric, B. Gomber, M. Grothe, M. Herndon, A. Hervé, P. Klabbers, A. Lanaro, A. Levine, K. Long, R. Loveless, A. Mohapatra, I. Ojalvo, T. Perry, G.A. Pierro, G. Polese, T. Ruggles, T. Sarangi, A. Savin, A. Sharma, N. Smith, W.H. Smith, D. Taylor, P. Verwilligen, N. Woods

†: Deceased

1: Also at Vienna University of Technology, Vienna, Austria

2: Also at CERN, European Organization for Nuclear Research, Geneva, Switzerland

3: Also at State Key Laboratory of Nuclear Physics and Technology, Peking University, Beijing, China

4: Also at Institut Pluridisciplinaire Hubert Curien, Université de Strasbourg, Université de Haute Alsace Mulhouse, CNRS/IN2P3, Strasbourg, France

5: Also at Skobeltsyn Institute of Nuclear Physics, Lomonosov Moscow State University, Moscow, Russia

6: Also at Universidade Estadual de Campinas, Campinas, Brazil

7: Also at Centre National de la Recherche Scientifique (CNRS) - IN2P3, Paris, France

8: Also at Laboratoire Leprince-Ringuet, Ecole Polytechnique, IN2P3-CNRS, Palaiseau, France

9: Also at Joint Institute for Nuclear Research, Dubna, Russia

- 10: Also at Suez University, Suez, Egypt
- 11: Now at British University in Egypt, Cairo, Egypt
- 12: Also at Cairo University, Cairo, Egypt
- 13: Now at Helwan University, Cairo, Egypt
- 14: Also at Zewail City of Science and Technology, Zewail, Egypt
- 15: Also at Université de Haute Alsace, Mulhouse, France
- 16: Also at Tbilisi State University, Tbilisi, Georgia
- 17: Also at RWTH Aachen University, III. Physikalisches Institut A, Aachen, Germany
- 18: Also at University of Hamburg, Hamburg, Germany
- 19: Also at Brandenburg University of Technology, Cottbus, Germany
- 20: Also at Institute of Nuclear Research ATOMKI, Debrecen, Hungary
- 21: Also at Eötvös Loránd University, Budapest, Hungary
- 22: Also at University of Debrecen, Debrecen, Hungary
- 23: Also at Wigner Research Centre for Physics, Budapest, Hungary
- 24: Also at Indian Institute of Science Education and Research, Bhopal, India
- 25: Also at University of Visva-Bharati, Santiniketan, India
- 26: Now at King Abdulaziz University, Jeddah, Saudi Arabia
- 27: Also at University of Ruhuna, Matara, Sri Lanka
- 28: Also at Isfahan University of Technology, Isfahan, Iran
- 29: Also at University of Tehran, Department of Engineering Science, Tehran, Iran
- 30: Also at Plasma Physics Research Center, Science and Research Branch, Islamic Azad University, Tehran, Iran
- 31: Also at Laboratori Nazionali di Legnaro dell'INFN, Legnaro, Italy
- 32: Also at Università degli Studi di Siena, Siena, Italy
- 33: Also at Purdue University, West Lafayette, USA
- 34: Now at Hanyang University, Seoul, Korea
- 35: Also at International Islamic University of Malaysia, Kuala Lumpur, Malaysia
- 36: Also at Malaysian Nuclear Agency, MOSTI, Kajang, Malaysia
- 37: Also at Consejo Nacional de Ciencia y Tecnología, Mexico city, Mexico
- 38: Also at Warsaw University of Technology, Institute of Electronic Systems, Warsaw, Poland
- 39: Also at Institute for Nuclear Research, Moscow, Russia
- 40: Now at National Research Nuclear University 'Moscow Engineering Physics Institute' (MEPhI), Moscow, Russia
- 41: Also at St. Petersburg State Polytechnical University, St. Petersburg, Russia
- 42: Also at Faculty of Physics, University of Belgrade, Belgrade, Serbia
- 43: Also at INFN Sezione di Roma; Università di Roma, Roma, Italy
- 44: Also at National Technical University of Athens, Athens, Greece
- 45: Also at Scuola Normale e Sezione dell'INFN, Pisa, Italy
- 46: Also at National and Kapodistrian University of Athens, Athens, Greece
- 47: Also at MTA-ELTE Lendület CMS Particle and Nuclear Physics Group, Eötvös Loránd University, Budapest, Hungary
- 48: Also at Institute for Theoretical and Experimental Physics, Moscow, Russia
- 49: Also at Albert Einstein Center for Fundamental Physics, Bern, Switzerland
- 50: Also at Mersin University, Mersin, Turkey
- 51: Also at Cag University, Mersin, Turkey
- 52: Also at Piri Reis University, Istanbul, Turkey
- 53: Also at Gaziosmanpasa University, Tokat, Turkey
- 54: Also at Adiyaman University, Adiyaman, Turkey
- 55: Also at Ozyegin University, Istanbul, Turkey

- 56: Also at Izmir Institute of Technology, Izmir, Turkey
- 57: Also at Marmara University, Istanbul, Turkey
- 58: Also at Kafkas University, Kars, Turkey
- 59: Also at Istanbul Bilgi University, Istanbul, Turkey
- 60: Also at Yildiz Technical University, Istanbul, Turkey
- 61: Also at Hacettepe University, Ankara, Turkey
- 62: Also at Rutherford Appleton Laboratory, Didcot, United Kingdom
- 63: Also at School of Physics and Astronomy, University of Southampton, Southampton, United Kingdom
- 64: Also at Instituto de Astrofísica de Canarias, La Laguna, Spain
- 65: Also at Utah Valley University, Orem, USA
- 66: Also at University of Belgrade, Faculty of Physics and Vinca Institute of Nuclear Sciences, Belgrade, Serbia
- 67: Also at Facoltà Ingegneria, Università di Roma, Roma, Italy
- 68: Also at Argonne National Laboratory, Argonne, USA
- 69: Also at Erzincan University, Erzincan, Turkey
- 70: Also at Mimar Sinan University, Istanbul, Istanbul, Turkey
- 71: Also at Texas A&M University at Qatar, Doha, Qatar
- 72: Also at Kyungpook National University, Daegu, Korea